DETERMINATION OF YEARLY PERFORMANCE AND DEGRADATION RATE OF ELECTRICAL PARAMETERS OF AMORPHOUS SILICON PHOTOVOLTAIC MODULE IN MINNA, NIGERIA

BY

MATTHEW, Samuel Oluwatobi

MTech/SPS/2017/6804

DEPARTMENT OF PHYSICS

FEDERAL UNIVERSITY OF TECHNOLOGY

MINNA

SEPTEMBER, 2021

DETERMINATION OF YEARLY PERFORMANCE AND DEGRADATION RATE OF ELECTRICAL PARAMETERS OF AMORPHOUS SILICON PHOTOVOLTAIC MODULE IN MINNA, NIGERIA

BY

MATTHEW, Samuel Oluwatobi

MTech/SPS/2017/6804

DEPARTMENT OF PHYSICS

FEDERAL UNIVERSITY OF TECHNOLOGY

MINNA

SEPTEMBER, 2021

DETERMINATION OF YEARLY PERFORMANCE AND DEGRADATION RATE OF ELECTRICAL PARAMETERS OF AMORPHOUS SILICON PHOTOVOLTAIC MODULE IN MINNA, NIGERIA

BY

MATTHEW, Samuel Oluwatobi

MTech/SPS/2017/6804

DEPARTMENT OF PHYSICS

FEDERAL UNIVERSITY OF TECHNOLOGY

MINNA

SEPTEMBER, 2021

DETERMINATION OF YEARLY PERFORMANCE AND DEGRADATION RATE OF ELECTRICAL PARAMETERS OF AMORPHOUS SILICON PHOTOVOLTAIC MODULE IN MINNA, NIGERIA

BY

MATTHEW, Samuel Oluwatobi

MTech/SPS/2017/6804

THESIS SUBMITTED TO THE POSTGRADUATE SCHOOL, FEDERAL UNIVERSITY OF TECHNOLOGY, MINNA, NIGERIA IN PARTIAL FULFILMENT OF THE REQUIREMENTS FOR THE AWARD OF THE DEGREE OF MASTERS OF TECHNOLOGY (MTech)

IN THE DEPARTMENT OF PHYSICS

SEPTEMBER, 2021

ABSTRACT

There is need for accurate knowledge of performance, degradation rate and lifespan of photovoltaic (PV) module in every location for an effective solar PV power system. Outdoor degradation analysis was carried out on amorphous silicon PV module rated 10 W using CR1000 software-based Data Acquisition System (DAS). The PV module under test and meteorological Sensors were installed on a metal support structure at the same test plane. The data monitoring was from 09:00 to 18:00 hours each day continuously for a period of four years, from (December 2014 to November 2018).The experiment was carried out near the Department of Physics, Federal University of Technology, Minna (latitude 09°37'N, longitude 06°32'E and 249 meters above sea level). The sensors were connected directly to the CR1000 Campbell Scientific data logger, while the module was connected to the logger via electronic loads. The logger was programmed to scan the load current from 0 to 1 A at intervals of 50mA every 5 minutes, and average values of short-circuit current, (I_{sc}), open-circuit voltage, (V_{oc}), current at maximum power, (I_{max}), voltage at maximum power, (V_{max}), power(P) and maximum power(P_{max}) obtained from the modules together with the ambient parameters are recorded and logged. Data download at the data acquisition site was performed every 7 days to ensure effective and close monitoring of the data acquisition system (DAS). At the end of each month and where necessary, hourly, daily and monthly averages of each of the parameters-solar irradiance, solar insolation, wind speed, ambient and module temperatures, and the output response variables (open-circuit voltage, V_{oc}, short-circuit current, I_{sc}, voltage at maximum power, V_{max}, current at maximum power, I_{max}, efficiency, Eff, and fill factor, FF) of the photovoltaic modules were obtained. Annual yearly averages of the performance variables were carried out to ascertain the performance, degradation rate and lifespan of the module. The module performance for the four years of study was compared with Standard Test Condition (STC) specifications. The maximum power achieved at 1000W/m^2 for the four years of study were 0.652W, 2.186W, 2.078W, and 1.812W representing 6.52%, 21.86%, 20.78% and 18.12% of the manufacturer's 10W specification. Module efficiency at 1000W/m^2 for the four years of study is 2.25%, 7.56%, 7.19%, and 6.27% respectively as against the manufacturers STC specification of 33%. Accordingly, Module Performance Ratios for the PV module investigated were 0.07, 0.23, 0.22 and 0.19 respectively. For the Rate of Degradation (RoD), it was observed that Open-Circuit voltage (V_{oc}), Short-Circuit Current (I_{sc}), Power-Output (P), Maximum Power (P_{max}), had an average yearly degradation rate of 0.73V, 0.010A, 0.040W, 0.050W respectively for the four years of study. To also determine the lifespan of the module, an empirically determined statistical model given as YEAR = 3.36 - 0.237 V_{oc} (v) - 71.5 I_{sc} (A) + 8.07 Power (W) was fitted to the observed data to predict the lifetime of the module at any given year.

TABLE OF CONTENTS

Cover page	
Title page	i
Declaration	ii
Certification	iii
Dedication	iv
Acknowledgement	v
Abstract	vi
Table of Content	vii
List of Figures	x
List of Tables	xiii
List of Plates	xiv
List of Abbreviations	xv
CHAPTER ONE	1
1.0 INTRODUCTION	1
1.1 Background of the study	1
1.2 Solar Energy	4
1.3 Solar Cells and Application	7
1.4 Statement of the Problem	11
1.5 Research Aim and Objectives	12
1.5.1 Aim	12
1.5.2 Objectives	12
1.6 Justification of the Research	13
1.7 Study Area	13

1.8 Scope and Limitations 17

CHAPTER TWO 18

2.0 LITERATURE REVIEW 18

2.1 Amorphous Silicon PV Module 18

2.2 Review of related Works 21

CHAPTER THREE 26

3.0 RESEARCH METHODOLOGY 26

3.1 Materials 26

3.2 Methods 26

3.2.1 Monitoring Stage 26

3.2.2 Data Analysis 29

CHAPTER FOUR 31

4.0 RESULTS AND DISCUSSION 31

4.1 Results 29

4.2 Statistical Analysis and Models 53

4.2.1 Descriptive Statistics: V_{oc} (V), I_{sc} (A), Power (W) 53

4.2.2 Inferential Statistics 54

CHAPTER FIVE 58

5.0 CONCLUSION AND RECOMMENDATIONS 58

5.1 Conclusion 58

5.2 Recommendation 59

REFERENCES 61

APPENDIX A 64

LIST OF FIGURES

Figure	Description	Page
1.1	Current-Voltage diagram of a PV cell	10
1.2	Different Mechanism influencing the I-V diagram	10
1.3	Map of the study area (Minna)	16
4.1	I-V Characteristics for amorphous silicon module as a function of global irradiance for year 2015	32
4.2	I-V Characteristics for the amorphous silicon module as a function of global irradiance for year 2016	32
4.3	I-V Characteristics for amorphous silicon module as a function of global irradiance for year 2017	33
4.4	I-V Characteristics for amorphous silicon module as a function of global irradiance for year 2018	33
4.5	Annual hourly average plot of short circuit current and open circuit voltage for the amorphous module in year 2015	35
4.6	Annual hourly average plot of power output and maximum power for the amorphous module in year 2015	35
4.7	Annual hourly average plot of short circuit current and open circuit voltage for the amorphous module in year 2016	36
4.8	Annual hourly average plot of power output and maximum power for the amorphous module in year 2016	37
4.9	Annual hourly average plot of short circuit current and open circuit voltage for the amorphous module in year 2017	38
4.10	Annual hourly average plot of power output and maximum power for the amorphous module in year 2017	38
4.11	Annual hourly average plot of short circuit current and open circuit voltage for the amorphous module in year 2018	39
4.12	Annual hourly average plot of power output and maximum power for the amorphous module in year 2018	40

4.13 Hourly average variation of short circuit current and open circuit voltage for amorphous module as a function of time for the month of January 2015 41

4.14 Hourly average variation of power output and maximum power for amorphous module as a function of time for the month of January 2015 41

4.15 Hourly average variation of short-circuit current and open-circuit voltage for amorphous module as a function of time for the month of August 2015 42

4.16 Hourly average variation of power output and maximum power for amorphous module as a function of time for the month of August 2015 42

4.17 Hourly average variation of short circuit current and open circuit voltage of amorphous module as a function of time for the month of January 2016 43

4.18 Hourly average variation of power output and maximum power of amorphous silicon module as a function of time for the month of January 2016 43

4.19 Hourly average variation of short circuit current and open circuit voltage of amorphous module as a function of time for the month of August 2016 44

4.20 Hourly average variation of power output and maximum power of amorphous silicon module as a function of time for the month of August 2016 44

4.21 Hourly average variation of short circuit current and open circuit voltage of amorphous module as a function of time for the month of January 2017 45

4.22 Hourly average variation of power output and maximum power of amorphous silicon module as a function of time for the month of January 2017 45

4.23 Hourly average variation of short circuit current and open circuit voltage of amorphous module as a function of time for the month of August 2017 46

4.24 Hourly average variation of power output and maximum power output of amorphous module as a function of time for the month of August 2017 46

4.25 Hourly average variation of short circuit current and open circuit voltage of amorphous module as a function of time for the month of January 47

4.26 Hourly average variation of power output and maximum power of amorphous silicon module as a function of time for the month of January 2018 47

4.27 Hourly average variation of short circuit current and open circuit voltage of amorphous module as a function of time for the month of August 2018 48

4.28 Hourly average variation of power output and maximum power of amorphous silicon module as a function of time for the month of August 2018 48

4.29 Variation of short circuit current and open circuit voltage as a function of years for amorphous module 52

4.30 Variation of power output and maximum power as a function of years for amorphous module 52

4.31 Line graph of the predicted value for the performance variables 57

LIST OF TABLES

Table	Description	Pages
3.1	Manufacturers specifications of the three solar modules at standard test conditions	29
4.1	Annual hourly averages of performance variables and ambient parameters for year one (2015)	34
4.2	Annual hourly averages of performance variables and ambient parameters for year two (2016)	36
4.3	Annual hourly averages of performance variables and ambient parameters for year three (2017)	37
4.4	Annual hourly averages of performance variables and ambient parameters for year four (2018)	39
4.5	Performance response for year 2015 at different irradiance levels	48
4.6	Performance response for year 2016 at different irradiance levels	48
4.7	Performance response for year 2017 at different irradiance levels	49
4.8	Performance response for year 2018 at different irradiance levels	49
4.9	Annual yearly averages of performance variables and ambient parameters for the amorphous module	51
4.10	Annual Average Rate of Degradation (RoD) of performance variables for the amorphous module	51
4.11	Mean, SE Mean, Standard deviation and variance	54
4.12	Coefficient of variable (Coef); T-test and P- value	55
4.13	Analysis of variance (ANOVA) for the Regression Equation	55
4.14	A twenty (20) years forecasting table	56

LIST OF PLATES

Plate	Description	Page
I	The Experimental Set up	28

LIST OF ABBREVIATIONS

A Area of the module

ANOVA Analysis of variance

a-Si Amorphous silicon

Coef Coefficients of variables

Ee irradiance

Eff Efficiency

FF Fill Factor

Hg Solar irradiance

I_{max} Current at maximum power point

I_{mp} Current at P_{max}

I_{sc} Short circuit current

MPR Module Performance Ratio

P Power output

P_{in} Solar power input

P_{max} Maximum power

PV Photovoltaic

RoD Rate of Degradation

RH Relative Humidity

STC Standard Test Conditions

SWE Stablear-Wronski effect

SE Standard Error

StDev Standard deviation

T_a	Ambient temperature
T_{mod}	Module Temperature
V_{mp}	Voltage at P_{max}
V_m	Voltage at maximum power point
WS	Wind Speed
Eff	Efficiency
V_{oc}	Open circuit voltage

CHAPTER ONE

1.0 INTRODUCTION

1.1 Background to the Study

A photovoltaic cell is an electrical device that converts the energy of light directly into electricity by the photovoltaic effect. It is a form of photoelectric cell, defined as a device whose electrical characteristics, such as current, voltage, or resistance, vary when exposed to light. Individual solar cell devices can be combined to form modules, and modules are combined to form solar panels. In basic terms a single junction silicon solar cell can produce a maximum open-circuit voltage of approximately 0.5 to 0.6 volts.

Solar cells are described as being photovoltaic, irrespective of whether the source is sunlight or an artificial light. They are used as a photo detector such asinfrared detectors, detecting light or other electromagnetic radiation near the visible range, or measuring light intensity. The operation of a photovoltaic (PV) cell requires three basic attributes:

- The absorption of light, generating either electron-hole pairs or excitons.
- The separation of charge carriers of opposite types.
- The separate extraction of those carriers to an external circuit.

In contrast, a solar thermal collector supplies heat by absorbing sunlight, for the purpose of either direct heating or indirect electrical power generation from heat. A "photo electrolytic cell" (photo electrochemical), on the other hand, refers either to a type of photovoltaic cell (like that developed by Edmond Becquerel and modern dye-sensitized solar cells), or to a device that splits water directly into hydrogen and oxygen using only solar illumination.(Ezewonra, 2016).

The ever increasing world energy demand, the fast depletion of fossil fuels and the unpredictable weather pattern due to global warming have prompted the world to look for alternative source of energy. New manufacturers have come up and new technologies have emerged to meet the high energy demand by consumers. While more manufacturers and new technologies are emerging, the reliability of solar PV modules becomes a critical performance measure for the success of the industry (Rong*et al.*, 2011). The performance of PV modules has been observed to gradually decrease with operation time (Dunlop and Halton, 2006). It is important to investigate the performance parameters of the modules. In order to have maximum sunlight conversion, the tilt and orientation of the modules should be maximized (Akachuku, 2011).

With rapid economic growth and improvement in living standards, there has been a marked increase in energy consumption in many third world countries. Most countries use fossil fuel, hydroelectric power and nuclear power as a source of energy. Nuclear and fossil fuels have adverse effects on the environment such as large amounts of greenhouse gases emissions and pollution from the burning of fossil fuel (René, 2005, Azhar and Abdul, 2012).

Since fossil fuel and nuclear sources of energy are not renewable, it is necessary to explore other sources of energy that are cost effective especially in the developing countries that rely heavily on imported fossil fuel. Renewable energy such as sunlight, wind tides and wave can be particularly suitable for developing countries especially in rural and remote areas where transmission and distribution of energy generated from fossil fuels can be difficult and expensive. Producing renewable energy locally can offer a viable alternative.

Technology advances are opening up a huge new market for solar power. Even though they are typically poor, these people have to pay far more for lighting than people in rich countries because they use inefficient kerosene lamps and stoves. Solar power costs half as much as lighting with kerosene. An estimated three million households get power from small solar panels (Duke *et al*., 1999).

The energy conversion efficiency of a PV module or array as a group of electrically connected PV modules in the same plane is defined as the ratio between electrical power conducted away from the module and the incidence power of the sun (Rakovect and Klemen., 2011). This conversion efficiency of photovoltaic (PV) modules by manufacturers is done under Standard Test Conditions (STC). The Standard Test Conditions are module temperature of $25^{o}C$, Irradiance of $1000W/m^2$ and Air mass of 1.5.

The orientation of PV modules determines their power output. This orientation is described by its azimuth and tilt angle. For fixed modules, the azimuth angle is the angle the modules make with the true North, when measured in a clockwise direction. The tilt angle is the angle that forms between the horizontal and the vertical axis of the PV module. It is the latitude at a given location. Many investigations have been carried out to determine the best tilt angle for PV systems.

Different PV module technologies now exist in the market. These include crystalline modules such as mono/single crystalline, poly/multi crystalline and amorphous modules. The modules available are rated by manufacturer depending on their power output such as 5Watts, 10Watts, 15 Watts. The choice of the module to use depends on the power output needed by the consumer and its efficiency. Photovoltaic (PV) modules are often considered as the most reliable elements in PV systems. However, PV module reliability data are not shown on commercial data sheets in the same way as it is with other products such as electronic devices and electric power supplies. Conversely, the high reliabilities associated with PV modules are indirectly reflected in the output power warranties usually provided in the industry, which range from 25-30 years. As a matter of fact, PV modules have a low return time, the exceptions being the catastrophic failures. The performance of PV modules decreases when deployed outdoors over time. After several years of operation, this decrease will affect PV module reliability (Manuel and Ignacio, 2008).In this study, it is therefore necessary to determine the yearly degradation rate of electrical parameters of amorphous silicon PV module and the findings can be used to investigate its stability and the reliability in any location.

1.2 Solar Energy

The earth is constantly lightened and warmed by the electromagnetic radiation from the sun. This energy warms the earth and atmosphere and sustains life on our planet. It is the most abundant source of energy that can be technically exploited by mankind with what we know today. The amount of solar energy reaching earth equals 4 x 10^6exajoules (EJ) per year. This is about ten thousand times the primary energy use of the world in 2007 (Chen, 2011).

The power of the electromagnetic radiation on a surface is called irradiance and is measured in watts per square meter (W/m^2). Irradiance depends on the radiant power of the sun, the distance between the earth and the sun, the angle at which it strikes the earth and on the atmospheric conditions.

The irradiance of the sun outside our atmosphere is fairly constant and changes only slightly dueto variations in the distance between sun and earth.The solar energy that reaches the earth’s surface varies greatly, depending on the geographical location, time, date and atmospheric conditions. This solar energy can be partially converted into electricity.

Solar energy is created at the core of the sun when hydrogen atoms are merged into helium by nuclear fusion. The core takes up an area from the sun’s centre to about a quarter of the star’s radius. At the core, gravity pulls all of the mass of the suns interior and produces strong pressure.

This pressure is much more adequate to force the fusion of atomic masses. For each second of the solar nuclear fusion process, 700 million tons of hydrogen is converted into the heavier atom helium. Since its formation 4.5 billion years ago, the sun has used up about half of the hydrogen found in its core. The solar nuclear process also produces enormous heat that makes the atoms to release photons. Temperature at the core are about 15 million degrees Kelvin (15 million ^{0}K). Each photon that is created travels about one micrometer before being absorbed by an adjacent gas molecule. The radiative surface of the sun, or photosphere, has an average temperature of about 5,800 Kelvin. A good number of the electromagnetic radiation released from the sun's surface sits in the visible band positioned at 500 nm (1 nm = 10^{-9} meters), though the sun also emits considerable energy in the ultraviolet and infrared bands, and small amount of energy in the radio, microwave, X ray and gamma ray bands. The total quantity of energy emitted from the sun's surface is about 63,000,000 Watts per square meter.

The sun hits the earth's surface at various angles ranging from 0^0 (just above the horizon) to 90^0 (directly overhead), as the earth is spherical in shape. The earth's surface obtains most of the radiant energy when the sun's rays are perpendicular. When the sun's rays are further slanted, they pass through the atmosphere to a longer distance, becoming more scattered and dispersed. As the earth is spherical, the cold Polar Regions do not receive high solar insolation, and also due to the slanting axis of rotation, the regions receive little or no sunlight throughout the year. The earth's surface gets more solar energy when the sun isinan elliptical orbit and is closer to the earth. The earth is closer to the sun when it is summer in the southern hemisphere and winter in the northern hemisphere. The 23.5 degrees tilt in the earth's axis of rotation is a very important factor in determining the amount of sunlight striking the earth at a specific place. Generally, the amount of insolation received at a particular place and time depends on the following factors:

i. Distance from the sun
ii. Duration of daily sunlight period
iii. Solar elevation or inclination of the solar rays to the horizon
iv. Transparency of the atmosphere towards the radiation and
v. Output of solar radiation

The first three of these factors are closely connected with revolution of the earth. It is to be noted here that the earth revolve around the sun in elliptic orbit and make one complete revolution in 365 days; simultaneously it spins about itself and completes one rotation in 24 hours. The average distance of the earth from the sun is 149.5 million km. The duration of daylight also varies with the latitude and season. The longer the daylight, the greater is the insolation received. In the solar region (i.e. region within solar activities of flares and winds) the duration of daylight is 24 hours during summer and minimum of zero in winter season (AgriInfo.in, 2013; http://www.innovateus.net, 2013).

1.3 Solar Cells and Applications

The photovoltaic effect was first experimentally demonstrated by French physicist A. E. Becquerel. In 1839, at the age of 19, experimenting in his father's laboratory, he built the world's first photovoltaic cell. However, it was not until 1883 that the first solid state photovoltaic cell was built, by Charles Fritts, who coated semiconductor selenium with an extremely thin layer of gold to form the junctions. In 1888 Russian Physicist AleksandrStoletov built the first photoelectric cell based on the outer photoelectric effect discovered by Heinrich Hertz earlier in 1887.

Albert Einstein explained the underlying mechanism of light instigated carrier excitation – the photoelectric effect – in 1905, for which he received the Nobel Prize in physics in 1921. Russell

Ohl patented the modern junction semiconductor solar cell in 1946, which was discovered while the researcher was working on the series of advances that would lead to the transistor.

The first practical photovoltaic cell was developed in 1954 at bell laboratories by Daryl Chapin, Calvin Souther Fuller and Gerald Pearson. At first, cells were developed for toys and other minor uses, as the cost of the electricity produced was very high; in relative terms, a cell that produced 1 watt of electrical power in bright sunlight cost about $250, and comparing to $2 to $3 per watt for a coal plant.

A quick introduction to solid state semiconductors is needed to understand the operating principles of a solar cell. A semiconductor is a material with an electrical conductivity between a conductor and an insulator. Its conductivity is defined by the ‘band gap’, the difference between the valence energy of bonded electrons and the conduction energy of free electrons. The most common semiconductor material is Silicon, and it forms the basis of most electronics (Twidell& Weir, 2006).

The current flow in intrinsic, or "pure" semiconductors is low. The conductive properties of thesilicon changes if certain impurities are added . Adding certain impurities is called "doping". The added impurities create either an electron surplus (n-type) or an electron deficit (p-type). The junction of a p-type and an n-type doped material creates so called diode, enabling conduction of electrons in one way but not the other way. A positive voltage applied to the junction will increase the electrical current, while a negative voltage will decrease the current. The relationship between current and voltage is described by the Shockley ideal diode equation (Twidell& Weir, 2006):

$$I = I_0 * [\exp\left(\frac{qV}{KT}\right) - 1](2.1)$$

Where Iis the current through a p-n junction, I_0 the saturation or recombination current, qtheelementary charge, V the applied voltage, kthe Boltzmann constant and Tabsolute temperature. A solar cell produces both a voltage and current when it is exposed to light. Electrons are knocked from their valence bonds leaving a 'hole' behind. A voltage pulls the electrons in one direction, which then migrate through the cell and through an electrical circuit after which they recombine with holes at the back contact of a solar cell. Under illumination, the total current,Iis the difference between the light generated current $I_L$and equation 2.1

$$I = I_L - I_0 * [\exp\left(\frac{qV}{KT}\right) - 1](2.2)$$

The short-circuit current $I_{sc}$is the current that would be measured, if there was no voltage across the cell. It is the maximum current that can be generated by a solar cell but without voltage no power is produced. The short-circuit current changes proportionally with irradiance and increases slightly with temperature.

If the voltage is increased, more and more recombination occurs within the cell. The maximumvoltage is called open-circuit voltage (V_{oc}) and at this point no power is produced because there is no current and all generated carriers recombine within the cell. When power is drawn from the cell the voltage decreases because fewer electrons accumulate. The open-circuit voltages changes only a little with irradiance but is very sensitive to temperature changes. A typical $V_{oc}$for silicon solar cells is 0.6V. The V_{oc}depends on temperature and on the ratio of the light-generated current and the recombination current as can be seen in equation 2.3 (Twidell& Weir, 2006),

$$V_{OC} = \frac{kT}{q} l_n(I_L/I_0+1) \qquad (2.3)$$

Where kis the Boltzmann constant and qthe elementary charge. An increase in temperature Tleads to a decrease in the open-circuit voltage because of the strong dependence of the saturation current I_0 on temperature. The I_0 depends on the intrinsic carrier concentration, which is proportional to the third power of absolute temperature (Muller*et al*; 2003). A rise in temperature leads to a strong increase in the intrinsic carrier concentration which increases the saturation current which ultimately leads to a drop in the V_{oc}.For each solar cell there is a current-voltage combination that has the highest yield. This is calledthe maximum power point (MPP). This point is characterized by the MPP voltage multiplied with the MPP current. A graphical representation of the current voltage relationship of a PV cell is shown in Figures 1.1 and 1.2.

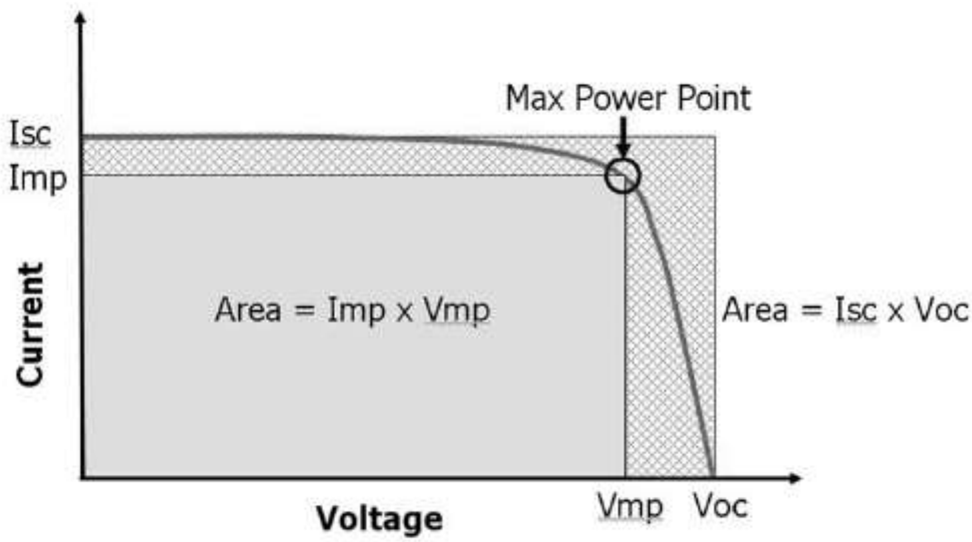

Figure 1.1: Current-voltage diagram of a PV cell. (Source: Solmetric, 2011)

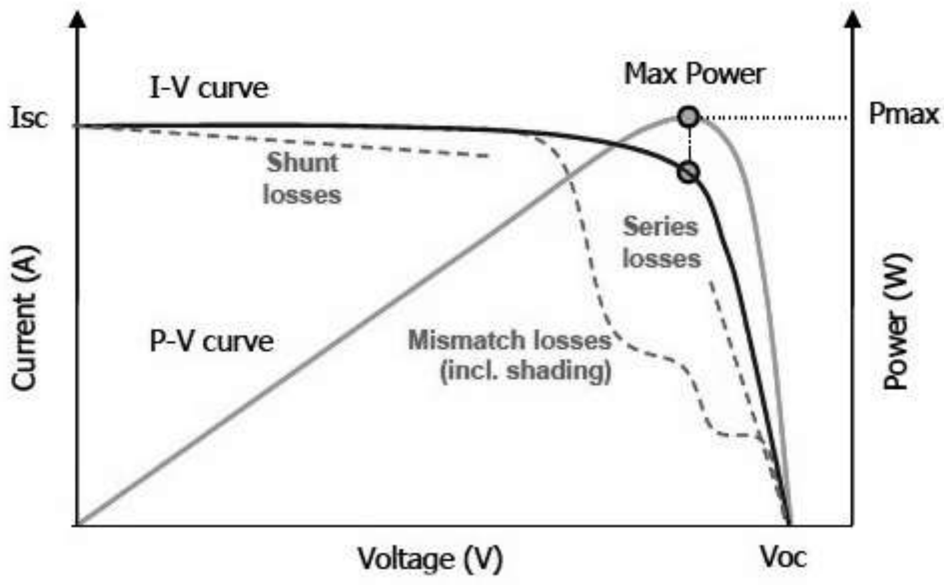

Figure 1.2: Different mechanism influencing the I-Vdiagram(Source: Solmetric, 2011).

The current-voltage, or I-V curve represent the combinations of current and voltage at which different mechanism influencing the I-V of a PV module or string can operate (Solmetric, 2011). A normal I-V curve can be divided into three areas: A very low slope starting at zero voltage, a ’bend’ or curve around the MPP and a steep slope between the MPP and the Voc. The I-V curve can look different, due to various reasons. An example can be seen in the upper plane of Figure 2.

The current can be lower than expected, for example due to soiling, shading or degradation ofthe module packaging. Another reason can be a decreased shunt resistance leading to current leaking away. The bend or curve around the MPP can change, for example due to corrosion and increased series resistance. The voltage can be lower than expected, for example due to increased temperatures caused by shaded cells (Solmetric, 2011).

The fill factor (FF) is also an important parameter in determining module performance. It is theratio of the MPP voltage times MPP current, and the open circuit voltage times the short circuit current:

$$\text{Fill factor (FF)} = I_{Max}V_{Max}/I_{SC}\ Voc \qquad (2.4)$$

The FF is also the ratio of the smooth gray area and the textured grey area in the lower plane of Figure 1.1

1.4 Statement of the Research Problem

Though we have lifetime of solar modules in literatures, in most cases, it is a projection from laboratory conditions which are quite different from real outdoor conditions. Even when the lifetime is from actual outdoor conditions, it is usually from foreign climatic zones other than ours. Consequently, laboratory conditions are suspect and contestable and actual outdoor evaluation, as regards degradation and lifetime are lacking in our local environment.These have necessitated the study of degradation rate and lifetime in our local environment since the atmospheric parameters that are responsible for the degradation change with locations. The result of this study will assist solar energy installers, planners and designers to have first hand information that will help in establishing an effective solar power system. Manufacturers do not state rate of degradations among their specifications, therefore, knowing their lifespan will help designers to design a good solar power system suitable for our local environment.

1.5 Aim and Objectives of the study

The aim of this research is to determine the rate of degradation of electrical parameters of amorphous silicon Photovoltaic modules as a result of atmospheric parameters in Minna, Niger State. The objectives are to:

i. characterise and evaluate the performance variables of the amorphous module using four years data.

ii. compare yearly performance variable of the amorphous module and deduce the rate of degradation using four years data

iii. deduce empirically determined model for prediction of yearly performance and life time of the amorphous module in our environment.

1.6 Justification of the Study

There are several types of photovoltaic (PV) modules from different manufacturers available in the market. The specifications provided in the manufacturers' data sheet indicate high performance and high reliability. These specifications are always measured at Standard Test Conditions (STC: module temperature = 25^o C, Irradiance = $1000W/m^2$ and Air mass = 1.5). That is not very representative of the real conditions in which the PV devices have to operate. Therefore, knowing the yearly performance together with the degradation rate and lifespan of amorphous PV module will assist researchers, policy makers, PV energy designers and installers in designing an effective PV power system best suited for our local environment. It will equally give the consumers first hand information on what to expect from their PV power system before installation, comparative cost advantage and also energy payback time.

1.7 Study Area

Solar energy availability on the earth's surface is site-dependent and varies throughout the year. It is only worthwhile installing solar radiation-based energy equipment in areas where one can be reasonably assured of adequate supply of such radiation. Minna is located on a location whose latitude is $09^o37'$N and longitude $06^o32'$ E, at altitude 249 metres above sea level and one of the Northern states of Nigeria that lie partially within the semi-arid Sahelian belt of West Africa. The climate of this zone is characterized by two distinct and well-defined seasons, namely wet and dry seasons. These seasons correspond to northern hemisphere summer and winter respectively.

The annual onset and cessation of the dry and wet seasons follow the quasi-periodic north-south to-and-fro movement of the inter-tropical convergence zone (ITCZ). The ITCZ demarcates the dry dust-laden north-east trade wind from the moisture-laden south-west wind. The dry season in the Sahel zone of Nigeria sets in about October each year and persists till about May of the next year. This is the period when the ITCZ is displaced

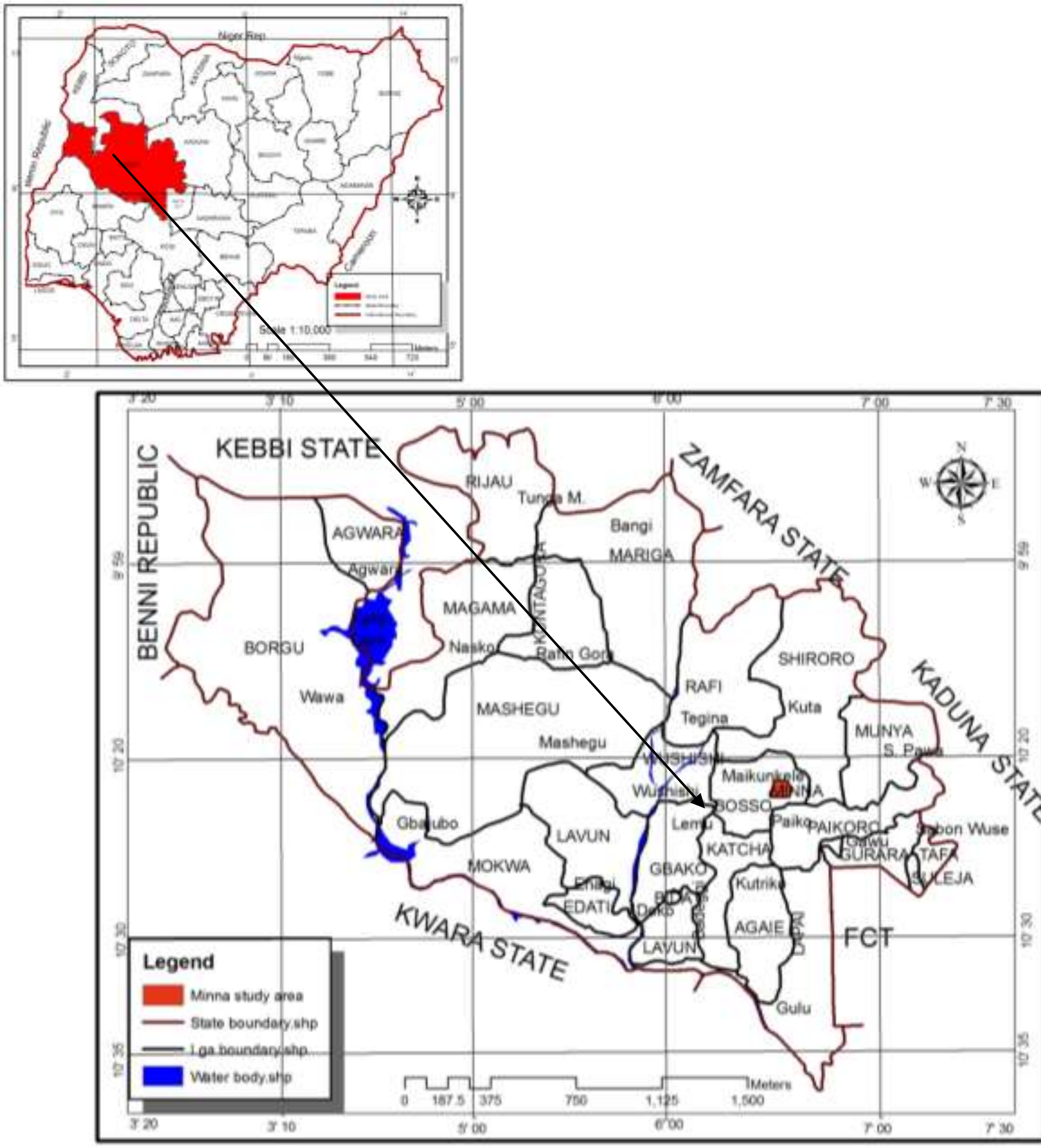

Figure 1.3: Study area (Minna).

Source: Niger State Ministry of Land and Housing to the south and the prevailing north-east trade wind transports large quantities of dust and smoke from biomass burning into the atmosphere over the entire region (Anuforom*et al*., 2007).

Dust and smoke aerosols' affect the climate system at local, regional and global scales in a number of ways. Due to its radiative impact, dust aerosols affects atmospheric temperature, thereby modifying the vertical temperature distribution in the troposphere as a result of the changes in heating and cooling rates at different altitudes (Carlson and Benjamin, 1980; Quijano, 2000). The stability of the atmosphere is thus affected. Some studies have suggested that dust and smoke aerosol in the atmosphere affects also photo synthetically active radiation (PAR) from the sun.

Average wet and dry season ambient temperature in Minna is 28.0^{o}C and 30.7^{o}C respectively, relative humidity is 70.8 and 39.9 respectively and wind speed is 1.68m/s for wet season and 1.82m/s for dry season.

However, Minna is endowed with annual average sunshine hours of about 9.00 hours. Similarly, it has an annual average daily solar irradiation of about 7.00kWh/m^{2}/day of energy from the sun (Bala*et al*; 2000). Therefore, Minna has the capacity for solar energy equipment.

1.8 Scope and Limitations

Photovoltaic (PV) modules degradation rates are location dependent because the atmospheric parameters that influence their degradation vary with location. Solar irradiance,ambient temperature, wind and relative humidity are the atmospheric parameters known to affect the performance of PV modules in any location on the earths' surface and the performance variables of a PV module are; open-circuit voltage, short circuit current, voltage at maximum power, current at maximum power, power output and maximum power.

However, different photovoltaic modules (monocrystalline silicon, polycrystalline silicon and amorphous silicon) respond differently to different atmospheric parameters. The study is only limited and within the context of yearly degradation rate of electrical parameters of amorphous silicon PV module in Minna.

CHAPTER TWO

2.0 LITERATURE REVIEW

2.1 Amorphous Silicon PV Module

Bell laboratories in 1974 produced the first amorphous silicon (a-Si) cell, having 0.2% efficiency. However the solar cell technology that has advanced rapidly since then aroused little interest about amorphous silicon at major conferences until the early 1980s.Among the thin film photovoltaic technologies currently in progress, amorphous silicon PV materials hold one of the most promising options for low cost solar modules. It is now the most mature and commercially viable technology. Amorphous silicon displays no atomic order regularity on any macroscopic scale, unlike crystalline silicon with its uniform lattice or grain of crystal structures. This disorder in amorphous silicon(a-Si) greatly limits the current flow even more than the grain boundaries do in polycrystalline materials. However, alloying it with hydrogen(a-Si:H), which provides acceptable conversion efficiencies, can diminish the disorder deficiencies in amorphous silicon. There are three major advantages associated with amorphous silicon alloys in solar cells, (Ezenwora, 2016).These include:

(a) They absorb solar radiation 40 times more efficiently than monocrystalline and polycrystalline silicon. A thickness of about only one micron is needed to absorb 90% of the available solar energy. This small amount of material needed saves significant costs.

(b) The materials can be produced at low temperatures and deposited on low cost substrates.

(c) The materials are amendable to large area automated production. Because of the disordered nature of a-Si:H material and its greater flexibility in tailoring improved photovoltaic properties and solar cell structures, it has an economic advantage over all other types of photovoltaic materials.

The presence of disorder and the incorporation of hydrogen also have a profound effect on the band gap and optical absorption. Alloying amorphous silicon with hydrogen increases the efficiency by lowering the band gap. The band gap for unalloyed amorphous silicon is about 1.7eV, which prevents it from absorbing photons from most of the suns spectrum. Investigations are still going on with the Silicon-Germanium and hydrogenated Silicon-Germanium(a-SiGe:H) to shrink the band gap to a level comparable to Gallium Arsenide band-gap which is generally considered to be nearly ideal for a solar cell material. The maximum possible conversion efficiency for a-SiGe:H is thought to be about 17%(Wronski,1985; Ezenwora, 2016).

A-Si:H does not behave like an indirect band gap semiconductor. It has the very optical absorption typically associated with direct band gap semiconductor. There is also no long-range order in the structural arrangement of atoms of amorphous silicon materials. The absence of this long-range order provides great flexibility in the design of different solar cell structures and in the manufacturing of large area monolithic modules. This large area deposition done at relatively low temperatures on a variety of substrates facilitates the mass production of a wide range of photovoltaic modules (Wronski*et al*., 2000; Ezewonra, 2016).

Efficient a-Si solar cell has a thickness of the order of 1um whereas a typical crystalline cell thickness is 100 to 200 um. This is because, the absorption coefficient in the amorphous silicon material, especially in the visible spectrum, is far larger than that in the crystalline silicon. A stable efficiency of 13% was recently achieved for a-Si cells as reported by (Yang,1997; Ezenwora, 2016). Also a stabilized efficiency of 9.5% for 1200 sqr cma-Si:H has been reported recently. This was possible by low temperature (180^{o}C) deposition of a-Si:H film while maintaining good opto-electronic properties(Neville, 1980;Ezenwora,2016).Hydrogenated amorphous silicon alloys are very promising thin-film materials for multijunction solar cells as well. Small laboratory scale cells (1 sqr cm) have gone from 1% to 2% efficiency in 1975 to over 13% efficiency between 1988 and 1997, while modules (about 1000 sqr cm), which were not in existence in 1975, have reached efficiencies of over 8%(Ohnishi et al.,1985). Current research efforts focus on developing and characterizing improved alloy materials for better performance (efficiency and stability) in multijunction cells. Many companies and Universities are currently involved in amorphous silicon research and development.

America also places heavy emphasis on amorphous silicon research and is concerned with advanced amorphous materials, device structures, thin-film preparation techniques and the characterization of electrical, optical and compositional properties. The Japanese have also focused their national PV program on the development of amorphous silicon. Several Japanese firms are now marketing such products as calculators, battery chargers and watches powered by amorphous silicon PV cells. The Japanese are also seriously exploring amorphous silicon for power applications. Further details about amorphous silicon cells and characteristics can be found in a classic literature edited by Kazmerski,1980; Ezenwora 2016).

2.2 Review of related works

Mon and Ross (1985) exposed Amorphous-Si cells, encapsulated in the polymers polyvinyl butyral (PvB) and ethylene vinyl acetate (EVA) for more than 1200 hours in a controlled 85% Relative Humidity environment, with a constant 500 volts applied between the cells and an aluminium frame. Plotting power output reduction versus charge transferred reveals that about

50% a-Si cell failures can be expected with the passage of 0.1 to 1.0 coulomb/cm of cell-frame edge length; this threshold is somewhat less than that determined for C-Si modules. Both visual and electrical data reveal many of the same degradation phenomena observed in C-Si studies. Patterns of degradation apparently unique to a-Si have also been observed. Among the latter are pinhole-like losses of silicon material and stress corrosion of the aluminium metallization layer.

Duke *et al*. (1999) conducted a survey on the field performance of amorphous Silicon (a-Si) photovoltaic modules in Kenya. The research revealed that small 10 to 14 Watt single junction amorphous Silicon (a-Si) modules dominate the market. Despite the commercial success there is substantial concern about the performance of single junction thin films amorphous silicon (a-Si) because the technology has an uneven quality and the uncertainty introduced by short term degradation usually occurs when this type of PV module is exposed to the sun.

Carr (2005) performed a detailed comparison of PV modules of different technologies and their implications for PV system design methods in Australia. The experiments revealed that the STC values quoted by the manufacturers for the PV modules do not necessarily match those observed in STC measurements. Van-Duke *et al*. (2006) studied the degradation of a thin-film hydrogenated single-junction amorphous silicon (a-Si:H) photovoltaic (PV) module . They investigated the different modes of electrical and physical degradation of a-Si:H PV modules by employing a degradation and failure assessment procedure used in conjunction with analytical techniques, including, scanning electron microscopy (SEM) and thermo-gravimetry. The investigation reveals that due to their thickness, thin films are very sensitive to the type of degradation observed. Moreover, the work deals with the problems associated with the module encapsulant, poly (ethylene-co-vinyl acetate) (EVA). The main objective of the study was to establish the influence of outdoor environmental conditions on the performance of a thin-film PV module comprising a-Si:H single-junction cells.

Domenico(2009) carried out a detailed study on the effect of current injection in amorphous silicon solar cells. A set of devices has been degraded and then annealed at different current intensities. Device performances during the whole experiment have been monitored by current/voltage characteristics and quantum efficiency curves. It has been found that annealing rate increases with current intensity, while stabilized photovoltaic parameters decreases. Time evolution of efficiency and short-circuit current during degradation has been reproduced by a numerical device modelling, resulting in a pronounced increase of defects near the p-i interface. The model also demonstrated that annealing results are not well reproduced if current-induced annealing is not energy selective.

Chantelle and Van-Dyke (2010) analyzed three commercial amorphous silicon modules manufactured by monolithic integration and consisting of three different technologies. These modules were deployed outdoors for 14 months and underwent degradation. All three modules experienced the typical light-induced degradation (LID) described by the Staebler–Wronski effect, and this was followed by further degradation. A 14 W single junction amorphous silicon module degraded by about 45% of the initial measured maximum power output (P_{MAX}) at the end of the study. A maximum of 30% of this has been attributed to LID and the further 15% to cell mismatch and cell degradation. The other two modules, a 64 W triple junction amorphous silicon module, and a 68 W flexible triple junction amorphous silicon module, exhibited LID followed by seasonal variation in the degraded P_{MAX}. The 64W module showed a maximum degradation in P_{MAX} of about 22%. This is approximately 4% more than the manufacturer allowed for the initial LID. However, the seasonal variation in P_{MAX} seems to be centred on the manufacturer's rating (±4%). The 68 W flexible modules have shown a maximum decrease in P_{MAX} of about 27%. This decrease is about 17% greater than the manufacturer allowed for the initial LID. A survey conducted by Duke *et al*. (1999) indicates that only 9% of PV module consumers think they know the brand of the modules they owned, and 15% of these respondents answered incorrectly. In addition, over 40% of the respondents would not guess about how long their modules would last. Less than 3% of the respondents knew whether they had an amorphous or crystalline solar module and only 6% of the respondents had an opinion about whether amorphous or crystalline modules existed.

Cornaro and Musella (2010) evaluated the performance of two PV modules, one polycrystalline and one amorphous during a medium term exposure at optimized tilt angle and did a complete characterization of weather conditions. The results showed that the polycrystalline module was highly stable with an average performance ratio (P.R) of 0.88. A seasonal trend in the monthly performance was observed due to the temperature effect on the module performance. The amorphous silicon module showed an effect of degradation in the first months of operation due to the Staebler- Wronski degradation effect.

Rong*et al*. (2011) reported that the degradation of solar photovoltaic modules is associated with the outdoor weather condition at the place of use. Agroui*et al*. (2011) evaluated the indoor and outdoor photovoltaic modules performances based on thin films solar cells. The tests showed that the Standard Test Condition (STC) values quoted by manufacturers for their amorphous modules do not match those observed in STC measurements. The modules were found to degrade within the first 8-10 weeks of exposure due to Staebler-Wronski effect on the amorphous silicon material.

Ezenwora*et al*. (2018) carried out an outdoor performance evaluation on three types of commercially available silicon PV modules rated 10 W each, using CR1000 software-based Data Acquisition System (DAS). The PV modules under test and meteorological sensors were installed on a metal support structure at the same test plane. The data monitoring was from 08.00 to 18.00 hours each day continuously for a period of one year, from December 2014 to November 2015. Maximum values of module efficiencies of 5.86% and 10.91% for the monocrystalline and polycrystalline modules were respectively recorded at irradiance of 375W/m^2, while the amorphous efficiency peaked at 3.61 % with irradiance of 536.5 W/m^2. At 1000 W/m^2 the efficiencies reduced to 3.30 %, 6.20 % and 2.25 % as against manufacturer's specifications of 46 %, 48 % and 33 % for the monocrystalline, polycrystalline and amorphous modules respectively.The maximum power output achieved for the modules at irradiance of 1000 W/m^2 were 0.711 W, 1.323 W and 0.652 W for the monocrystalline, polycrystalline and amorphous PV modules, respectively. Accordingly, Module Performance Ratios for the PV modules investigated were 0.07, 0.13 and 0.07, respectively. The rate of variation of module response variables with irradiance and temperature was determined using a linear statistical model given as Y= a + bHg+ c Tmod. The approach performed creditably well when compared with measured data.

CHAPTER THREE

3.0 MATERIALS AND METHODS

3.1 Materials

The Solar Module:

The brand (model/make) used is SLP 10-12/China for the three kinds of commercially available PV modules; single crystal, multi-crystal and non-crystal silicon.

Li-200SA M200 Pyranometer

HC2S3-L Rotronic HygroClip2

03002-L RM Young Wind Sentry Set

110PV-L Surface-Mount Temperature Probe

Electronic Loads (3)

CR 1000 Campbell Scientific Data Logger

Laptop Personal Computer

3.2 Methods

3.2.1 Monitoring Stage

The degradation rate of the amorphous silicon PV module was monitored in Minna environment, using CR1000 software-based data logging system with computer interface. The PV modules under test, and meteorological sensors, were installed on support structure at the same test plane, at about three meters of height, so as to ensure adequate exposure to insolation and enough wind speed, since wind speed is proportional to height. The elevation equally ensures that the system is free from any shading from shrubs and also protected from damage or interference by intruders. Also, the whole experimental set up is secured in an area of about four meters in diameter. The modules are tilted at approximately 10^o (since Minna is on latitude 09^o 37$'$N) to horizontal and south-facing to ensure maximum insolation.

The data monitoring was from 9.00am to 6.00pm local time, each day continuously for a period of four years, spanning from December 2014 to November 2018. The experiment was carried out at the Bosso campus of the Federal University of Technology, Minna (latitude 09^{o}37'N, longitude 06^{o}32'E and 249 meters above sea level). The sensors are connected directly to the CR1000 Campbell Scientific data logger, while the module is connected to the logger via electronic loads. The logger was programmed to scan the load current from 0 to 1 A at intervals of 50mA every 5 minutes, and average values of short-circuit current, I_{sc}, open-circuit voltage, V_{oc}, current at maximum power, I_{max}, voltage at maximum power, V_{max}, power and maximum power obtained from the modules together with the ambient parameters are recorded and logged. Data download at the data acquisition site was performed every 7 days to ensure effective and close monitoring of the data acquisition system (DAS). At the end of each month and where necessary, hourly, daily and monthly averages of each of the parameters-solar irradiance, solar insolation, wind speed, ambient and module temperatures, and the output response variables (open-circuit voltage, (V_{oc}), short-circuit current, (I_{sc}), voltage at maximum power, (V_{max}), current at maximum power, (I_{max}), efficiency, (Eff), and fill factor, FF) of the photovoltaic modules were obtained.

The global solar radiation was monitored using Li-200SA M200 Pyranometer, manufactured by LI-COR Inc.USA, with calibration of 94.62 microamperes per 1000W/m^2. The ambient temperature and relative humidity was monitored using HC2S3-L RotronicHygraClip2 temperature/relative humidity probe, manufactured in Switzerland. Wind speed was monitored using 03002-L RM Young Wind Sentry Set. And module temperature was monitored using

110PV-L Surface-Mount Temperature probe. All sensors are installed in the CR1000 Campbell Scientific data logger with measurement and control module in plate 1.

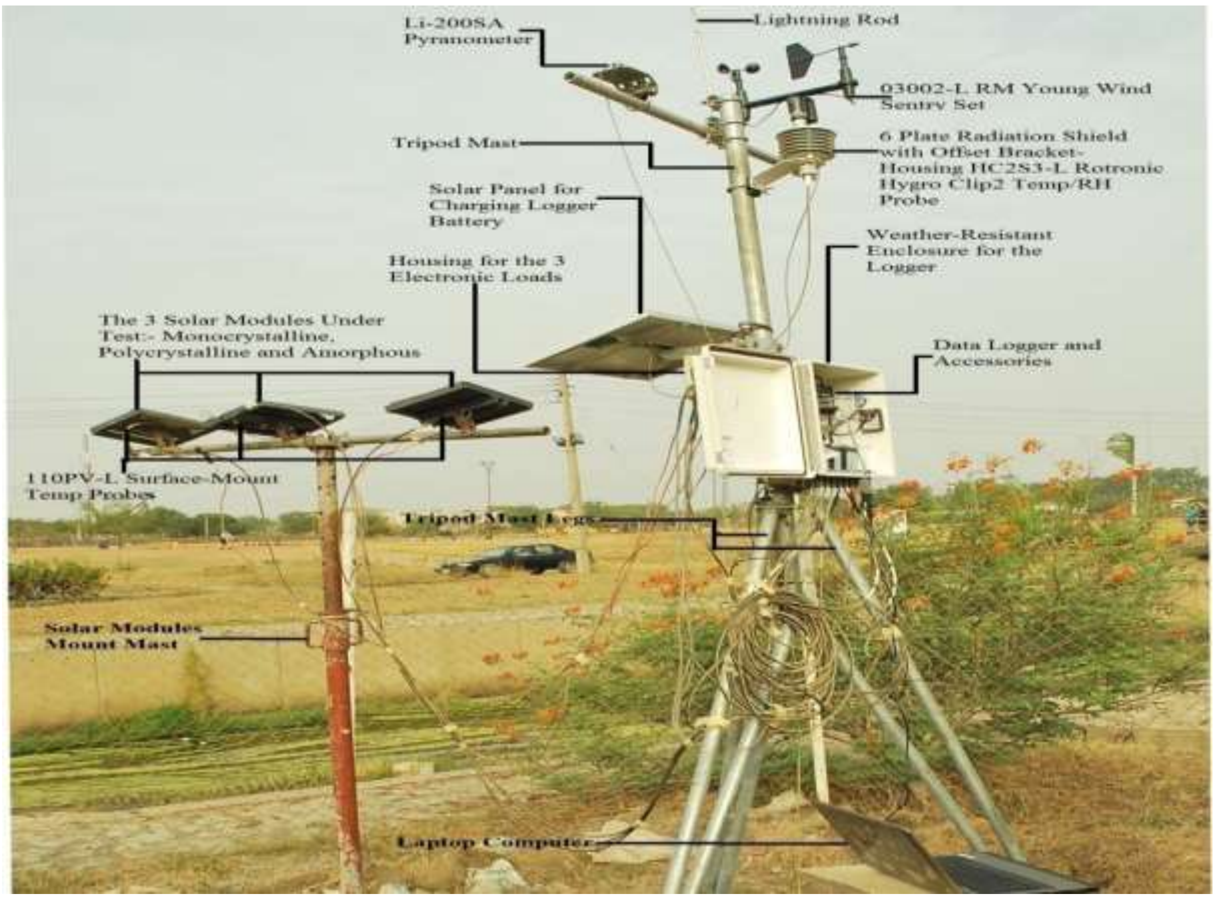

Plate 1: The Experimental set up (Near Physics Department, FUT Minna).

Table 3.1: Manufacturer's Specifications of Amorphous silicon module at Standard Test Conditions

Cell technology	No of cells per Module	Max. Rated Power (W)	Max. Rated Voltage (V)	Max. Rated Current (A)	Open-Circuit Voltage (V)	Short-Circuit Current (A)	Module Dimensions (m x m)	Cell Dimensions (m x m)	Total Surface Area of Cells (m^2)	Model/ Make	Eff (%)
Amorphous Module	17 Cells in singles series string	10	17.4	0.55	21.2	0.62	0.30 x 0.12	0.1 x 0.017	0.0289	SLP 10.12 / China	33*

3.2.2 Data analysis

Degradation rate of the amorphous module by solar irradiance was investigated in terms of open-circuit voltage, (V_{oc},) short-circuit current, (I_{sc},) voltage at maximum power, (V_{max}), current at maximum power, (I_{max}), efficiency, (Eff,) and fill factor, (FF). Fill factor, (FF), Efficiency, (EFF), and Module Performance Ratio (MPR) were evaluated using the following expressions:

$$\mathrm{FF} = \mathrm{ImaxVmax} \,/\, \mathrm{IscVoc} \qquad (3.1)$$

$$\mathrm{EFF} = {}^{\mathrm{ImaxVmax}}/_{\mathrm{Pin}} = {}^{\mathrm{IscVocFF}}/_{\mathrm{AEe}} \qquad (3.2)$$

MPR = Effective Efficiency / Efficiency at STC (3.3)

where P_{in} = power input

A= Area of the Amorphous Module

Ee = Solar Irradiance

In order to determine the Rate of Degradation (ROD), a statistical analysis was performed on the observed data with the aid of statistical package; Minitab 17 and Microsoft excel used for prediction of performance variables are presented. Multiple regression models, analysis of variance (ANOVA) and twenty years forecast using the model developed was done with the aim of establishing the statistical significant relationship between the variables thereby predicting the lifetime of the amorphous module. The regression equation is

$$Y = a - bV_{oc} - cI_{sc} + dPower \quad (3.4)$$

The I-V curves were produced by plotting current against voltage produced by the logger in scanning the electronic load current from 0 to 1A at intervals of 50mA. The maximum power point, P_{max}, which is the operating point of the module, was equally recorded by the logger. This maximum power point also corresponds to the largest area of the rectangle that fits the curve. The current and voltage at this point are I_{max} and V_{max} respectively.

CHAPTER FOUR

4.0 RESULTS AND DISCUSSION

Results from the characterisation and performance evaluation of the amorphous silicon module as well as the rate of degradation using four years data are discussed here. Discussion of these results and a statistical model used to predict the life time of the amorphous silicon module will equally be presented thereafter.

4.1 Results

Daily hourly data considered were from 9:00am to 6:00pm local time and, where necessary, hourly, daily, monthly and annual averages were computed within these hours.The amorphous module under study using four years data does not depict diode characteristics that are usually associated with solar modules. The reason is because the manufacturer's specifications are particularly too unrealistic that its actual performance is far below the range of electronic load designed for it, which was based on the specification of the manufacturer. It was discovered that the manufacturer's specification current was 0.62 amperes, but no year was able to deliver up to 0.1 amperes of current for the four years of study and this explains the sudden descent in the characteristic curve immediately it was loaded giving slanting lines instead of a curve that is normal to other types of modules (monocrystalline and polycrystalline). Figures 4.1 to 4.4 show the output characteristics of the amorphous silicon PV module as a function of global irradiance using four years data. These output characteristics are expressed in form of I-V curves.

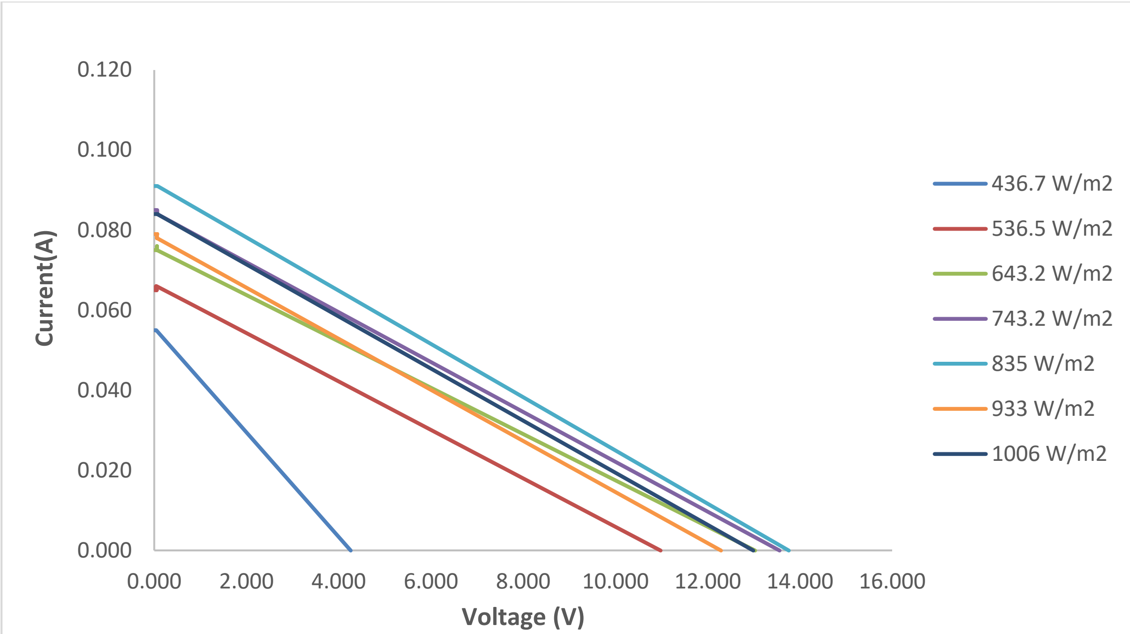

Figure 4.1: I-V Characteristics of the amorphous silicon module as a function of global irradiance for the first year.

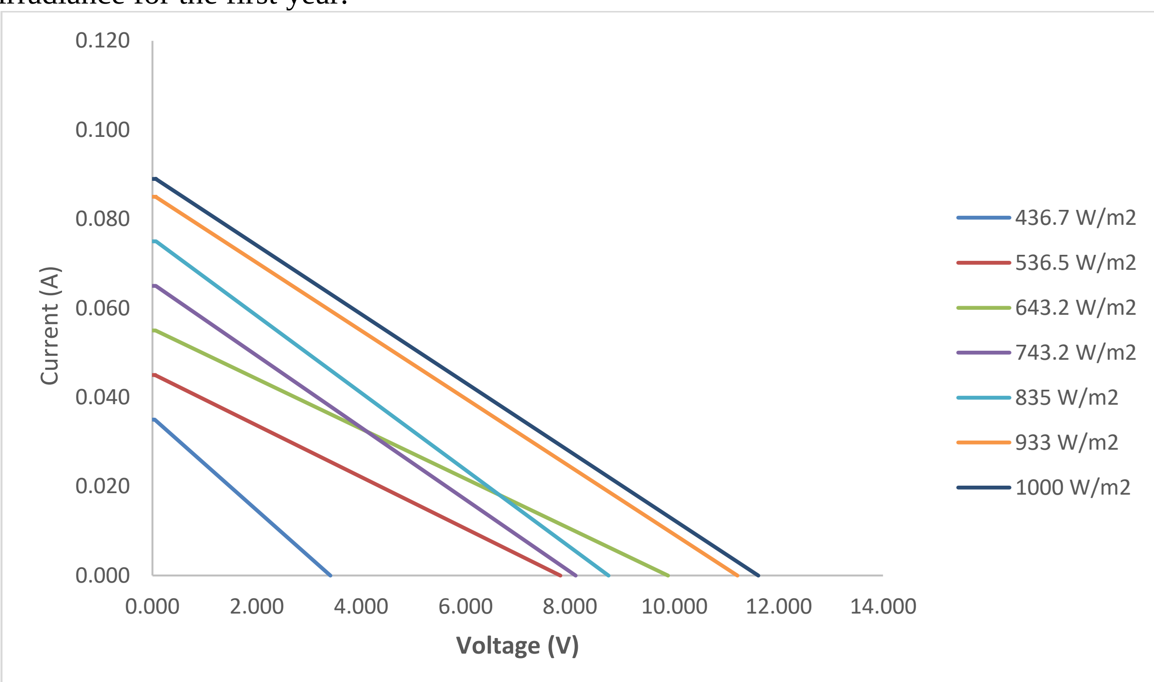

Figure 4.2: I-V Characteristics of the amorphous silicon module as a function of global irradiance for the second year.

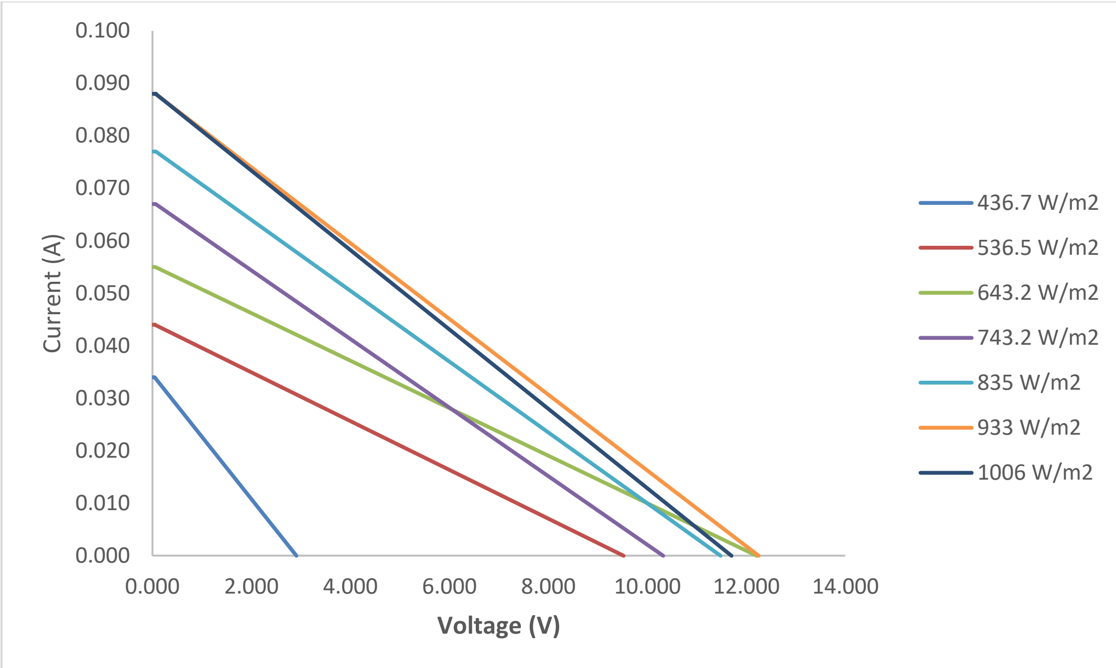

Figure 4.3: I-V Characteristics of the amorphous silicon module as a function of global irradiance for the third year.

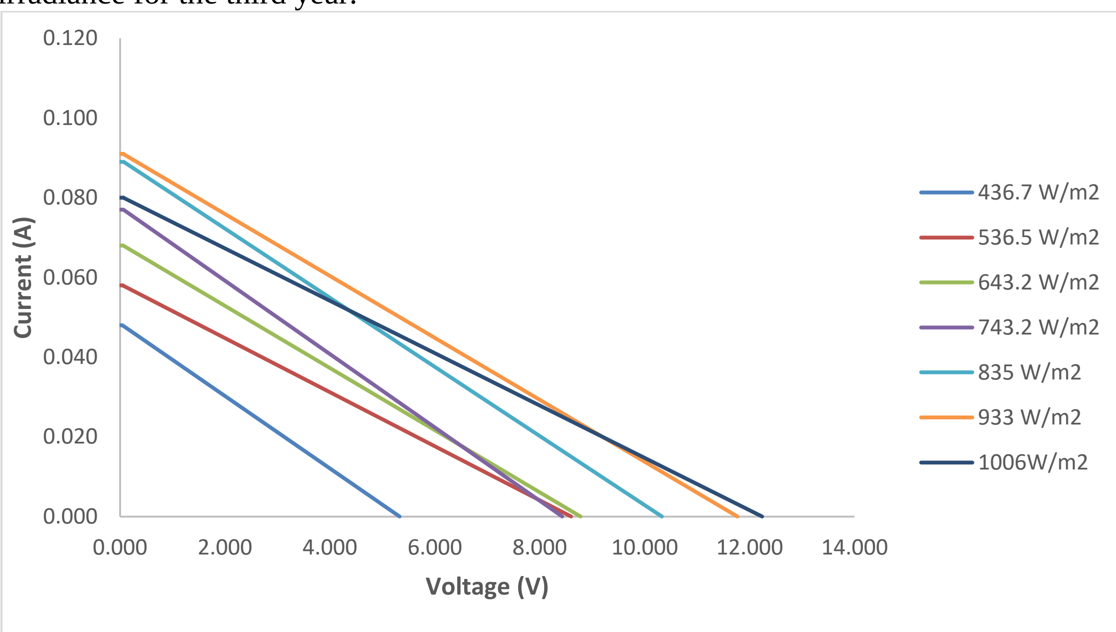

Figure 4.4: I-V Characteristics of the amorphous silicon module as a function of global irradiance for the fourth year.

The output characterization of solar modules (monocrystalline, polycrystalline and amorphous) is usually based on trends of the I-V curve as a function of global irradiance. The amorphous module under study using four years data does not depict diode characteristics that are usually associated with solar modules. The reason is because the manufacturer's specifications are particularly too unrealistic that its actual performance is far below the range of electronic load designed for it, which was based on the specification of the manufacturer. It was discovered that the manufacturer's specification current was 0.62 amperes, but no year was able to deliver up to 0.1 amperes of current for the four years of study and this explains the sudden descent in the characteristic curve immediately it was loaded giving slanting lines instead of a curve that is normal to other types of modules (monocrystalline and polycrystalline) as seen in Figures 4.1 to 4.4.

Annual hourly average values of the module performance variables and ambient parameters for the four years data collected are shown in Tables 4.1 – 4.4 while the annual hourly average plots of the performance variables are shown in Figures 4.5 – 4.12.

Table 4.1: Annual hourly averages of performance variables and ambient parameters for year one (2015).

T(Hours)	WS(m/s)	$T_a(^0C)$	RH(%)	$T_{mod}(^0C)$	$H_g(W/m^2)$	V_{oc} (v)	I_{sc} (A)	P(W)	P_{max}(W)
9 AM	1.94	21.3	56.6	30.2	419	0.37	0.029	0.019	0.022
10 AM	1.98	23.1	54.5	32.7	561	2.01	0.039	0.105	0.142
11 AM	1.87	24.5	51.9	35.0	661	4.74	0.045	0.253	0.355
12 PM	1.80	25.5	49.4	36.9	705	6.79	0.047	0.362	0.534
1 PM	1.66	26.4	46.7	38.2	698	7.16	0.048	0.383	0.563
2 PM	1.61	27.1	45.1	38.3	611	5.89	0.046	0.316	0.433
3 PM	1.50	27.3	43.8	37.7	489	2.12	0.043	0.121	0.147
4 PM	1.40	27.4	43.4	36.2	318	0.07	0.031	0.013	0.013
5 PM	1.15	26.5	44.1	33.6	137	0.02	0.014	0.004	0.005
6 PM	0.94	25.3	45.6	31.8	58	0.01	0.006	0.000	0.000

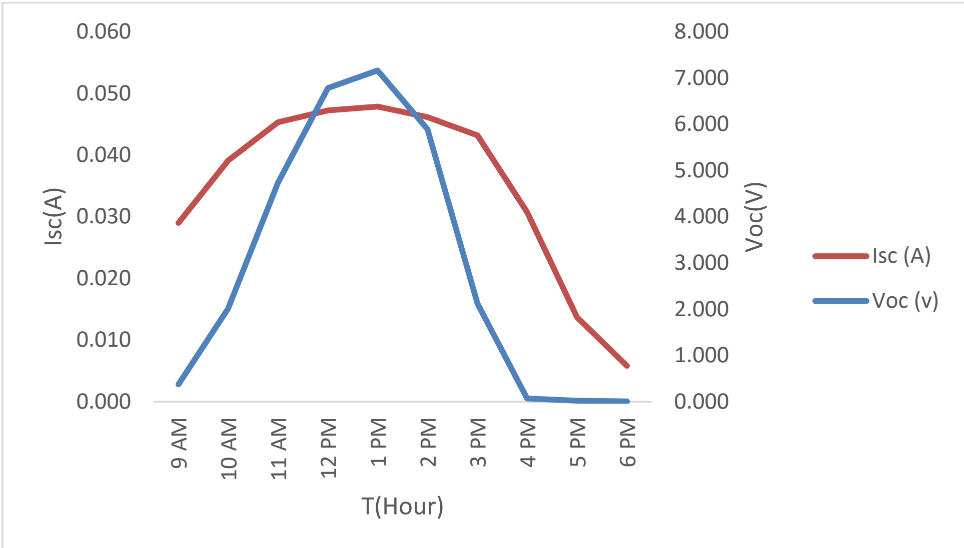

Figure 4.5: Annual hourly average plot of short-circuit current and open circuit-voltage for the amorphous module in year 2015.

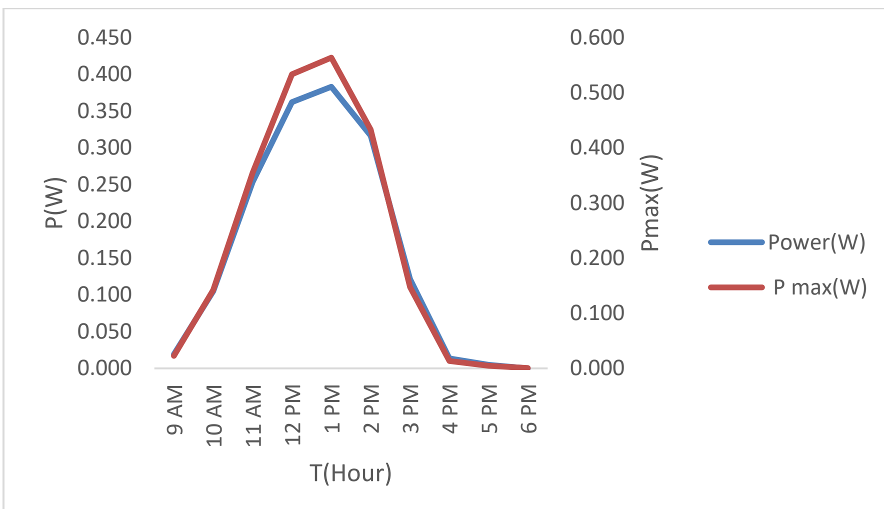

Figure 4.6: Annual hourly average plot of power output and maximum power for the amorphous module in year 2015.

Table 4.2: Annual hourly averages of performance variables and ambient parameters for year two (2016).

T(Hours)	WS(m/s)	$T_a(^0C)$	RH(%)	$T_{mod}(^0C)$	$H_g(W/m^2)$	V_{oc} (v)	I_{sc} (A)	P(W)	P_{max}(W)
9 AM	1.86	27.6	60.1	30.0	414	0.11	0.006	0.008	0.010
10 AM	1.84	29.1	56.4	32.8	566	1.93	0.024	0.158	0.203
11 AM	1.76	30.5	52.9	35.3	663	4.71	0.046	0.425	0.516
12 PM	1.71	31.6	49.9	37.2	723	6.03	0.055	0.557	0.671
1 PM	1.60	32.4	47.4	38.3	708	5.77	0.056	0.519	0.642
2 PM	1.53	32.9	45.4	38.6	641	3.76	0.047	0.290	0.390
3 PM	1.45	33.1	44.6	37.9	518	0.82	0.030	0.046	0.082
4 PM	1.31	33.0	44.4	36.4	338	0.03	0.019	0.002	0.003
5 PM	1.12	32.2	46.6	33.5	148	0.01	0.011	0.001	0.001
6 PM	0.92	31.4	49.3	31.5	61	0.01	0.004	0.001	0.001

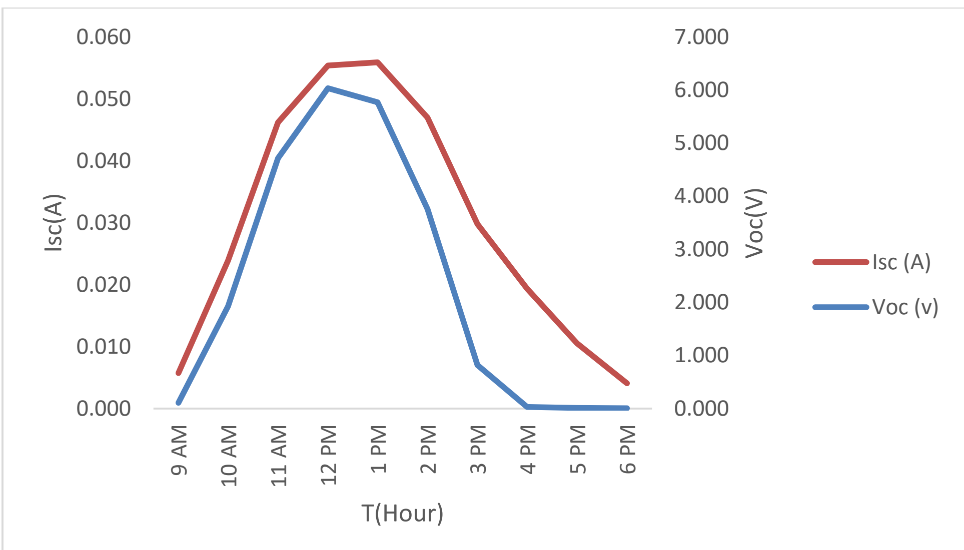

Figure 4.7: Annual hourly average plot of short-circuit current and open circuit-voltage for the amorphous module in year 2016.

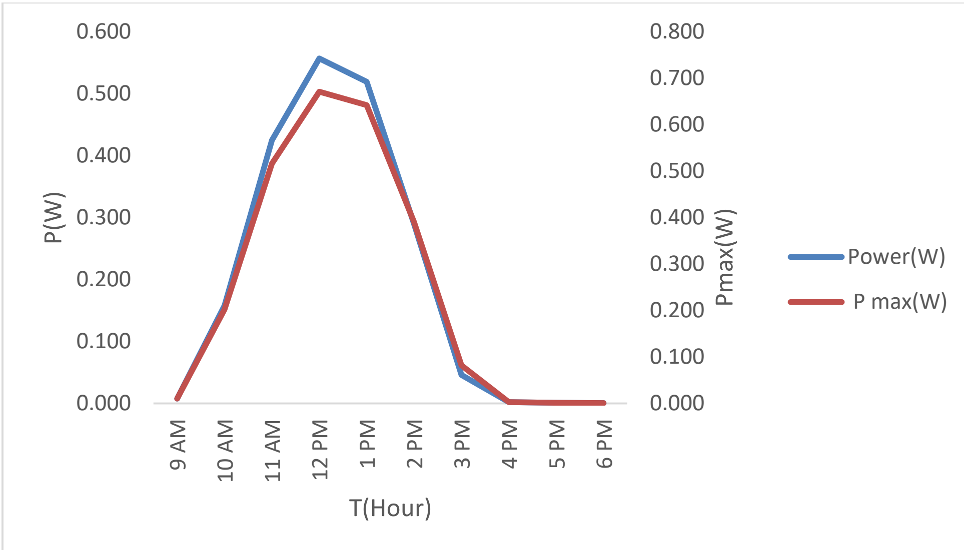

Figure 4.8: Annual hourly average plot of power output and maximum power for the amorphous module in year 2016.

Table 4.3: Annual hourly averages of performance variables and ambient parameters for year three(2017).

T(Hours)	WS(m/s)	T_a(^{0}C)	RH(%)	T_{mod}(^{0}C)	H_g(W/m^2)	V_{oc} (v)	I_{sc} (A)	P(W)	P_{max}(W)
9 AM	1.64	28.5	56.6	31.0	409	0.13	0.003	0.009	0.013
10 AM	1.63	30.1	53.2	33.9	552	1.50	0.014	0.148	0.183
11 AM	1.54	31.5	50.0	36.4	648	3.17	0.023	0.362	0.416
12 PM	1.48	32.6	47.4	38.3	694	3.87	0.041	0.477	0.538
1 PM	1.41	33.3	45.0	39.4	684	3.84	0.048	0.483	0.547
2 PM	1.27	33.7	43.2	39.4	614	2.67	0.041	0.316	0.363
3 PM	1.17	33.9	42.1	38.6	492	0.69	0.023	0.069	0.082
4 PM	1.07	33.7	42.3	36.9	322	0.03	0.013	0.003	0.003
5 PM	0.89	33.0	44.3	34.0	144	0.01	0.003	0.001	0.001
6 PM	0.75	32.2	47.0	32.0	62	0.01	0.005	0.001	0.001

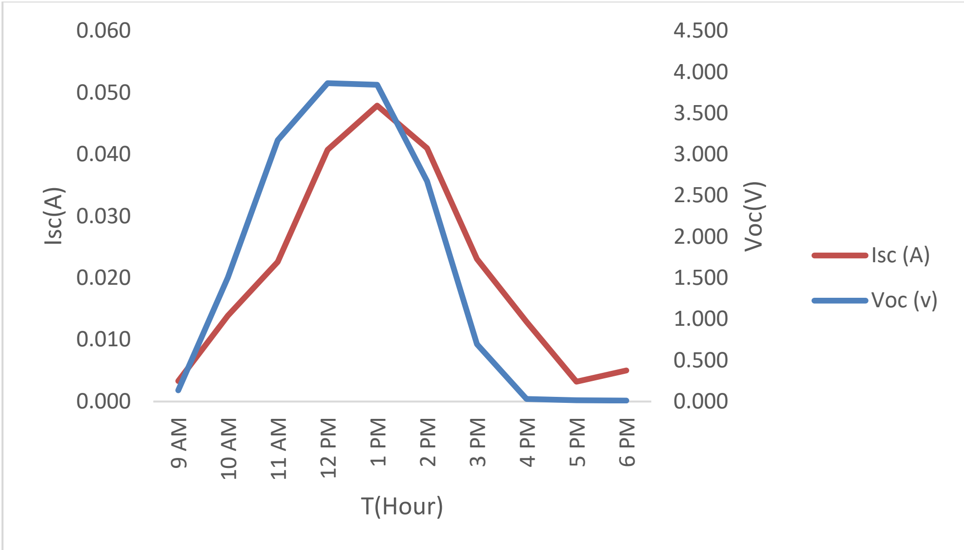

Figure 4.9: Annual hourly average plot of short-circuit current and open circuit-voltage for the amorphous module in year 2017.

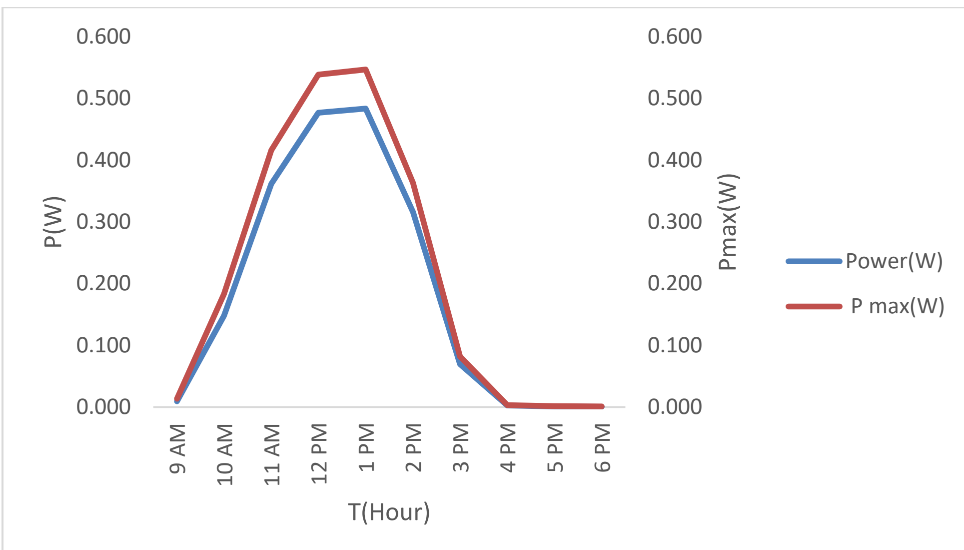

Figure 4.10: Annual hourly average plot of power output and maximum power for the amorphous module in year 2017.

Table 4.4: Annual hourly averages of performance variables and ambient parameters for year four (2018).

T(Hours)	WS(m/s)	$T_a(^0C)$	RH(%)	$T_{mod}(^0C)$	$H_g(W/m^2)$	V_{oc} (v)	I_{sc} (A)	P(W)	P_{max}(W)
9 AM	1.31	28.9	64.8	30.4	380	0.13	0.000	0.008	0.011
10 AM	1.37	30.5	60.8	33.3	519	1.43	0.001	0.089	0.130
11 AM	1.21	32.1	56.9	36.1	624	3.41	0.004	0.228	0.313
12 PM	1.15	33.3	53.7	38.0	670	4.22	0.025	0.346	0.432
1 PM	1.07	34.0	50.7	39.2	674	4.26	0.034	0.367	0.464
2 PM	0.97	34.3	48.3	39.3	603	2.78	0.026	0.213	0.285
3 PM	0.89	34.3	47.2	38.4	474	0.44	0.008	0.025	0.043
4 PM	0.72	34.0	46.8	36.7	316	0.02	0.001	0.002	0.002
5 PM	0.61	33.3	48.7	33.7	143	0.01	0.001	0.001	0.001
6 PM	0.48	32.5	51.0	31.6	62	0.01	0.002	0.001	0.001

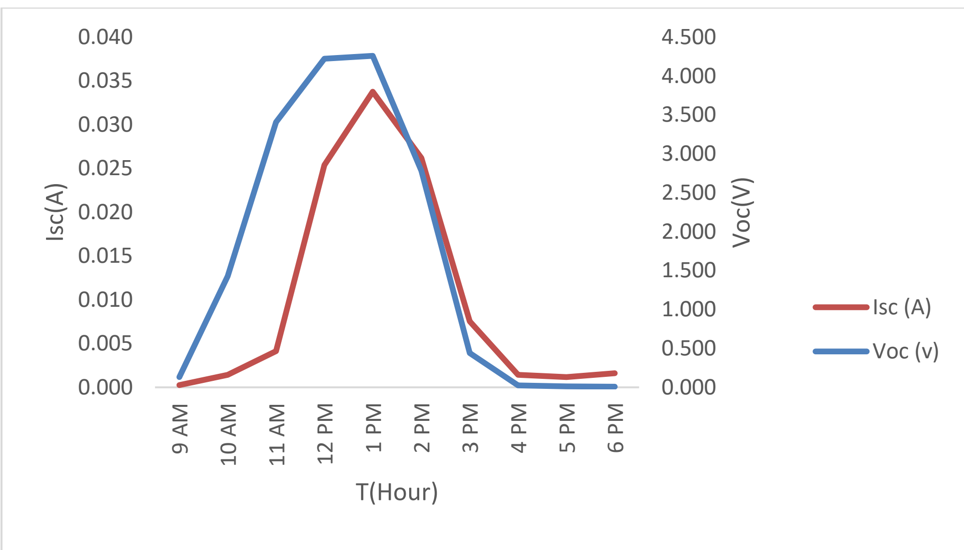

Figure 4.11: Annual hourly average plot of short-circuit current and open circuit-voltage for the amorphous module in year 2018.

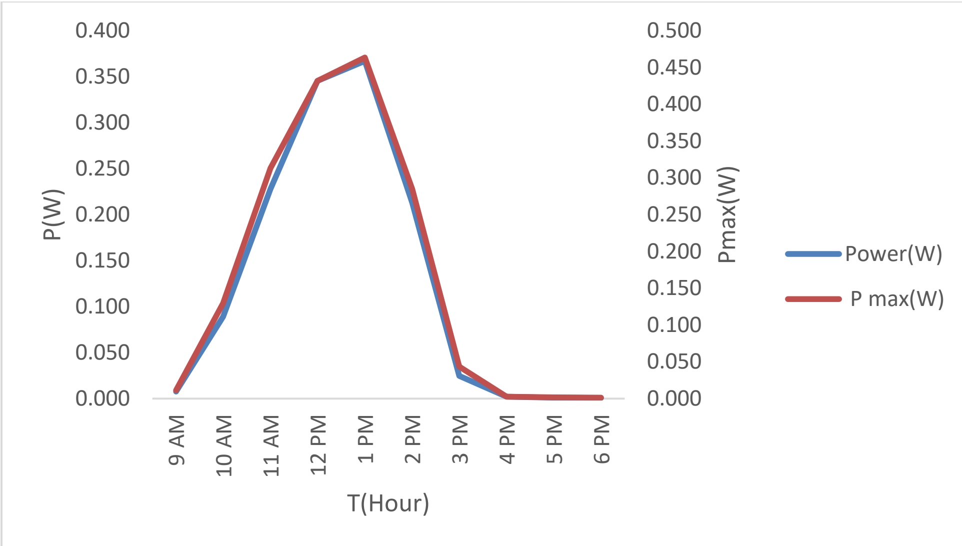

Figure 4.12: Annual hourly average plot of power output and maximum power for the amorphous module in year 2018.

It was discovered from tables 4.1 - 4.4 that the all performance variables of the amorphous module are seen to peak between the hours of 12pm and 1pm local time for the four years of study. For the ambient parameters, solar irradiance (Hg) peak time is at 12pm while ambient temperature (T_a) peaked between 2pm and 4pm local time for the four years of study respectively. Similarly, for wind speed (WS), its peak time is seen between 9am and 10am while relative humidity (RH) was equally observed to peak at 9am local time throughout the four years in the minna local environment. Also, it was closely observed that module temperature (T_{mod}) peaked at 2pm local time throughout the period of study as shown intables 4.1 - 4.4.

Monthly hourly averages of the performance variables (open circuit voltage, short-circuit current, power output, maximum power) are investigated using four years data collected and the plots for a typical dry season month (January) and a typical rainy season month (August) for each year (2015 – 2018) are shown in Figures 4.13 – 4.27.

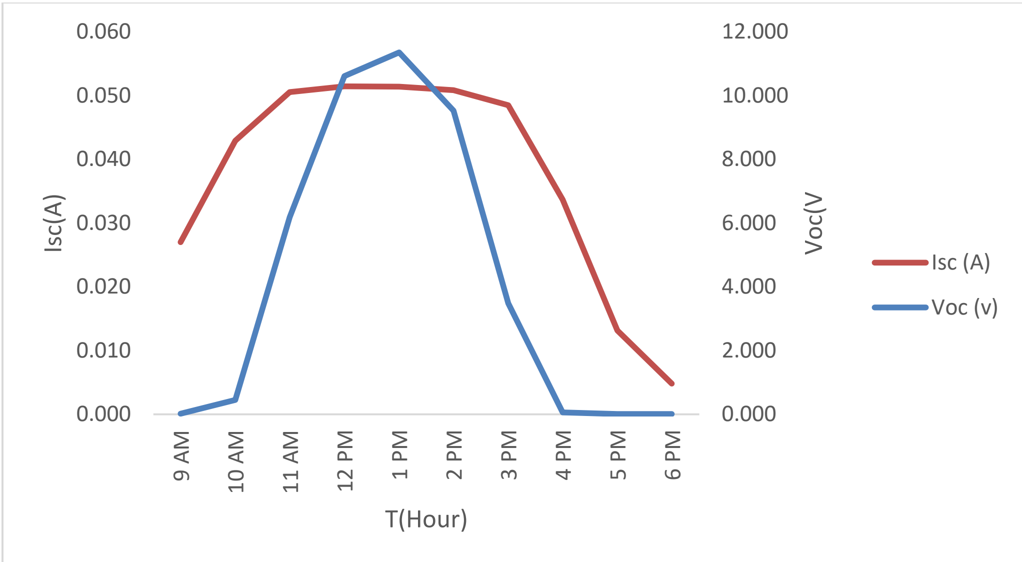

Figure 4.13: Hourly averages variation of short-circuit current and open-circuit voltage of amorphous silicon module as a function of time for the month of January 2015.

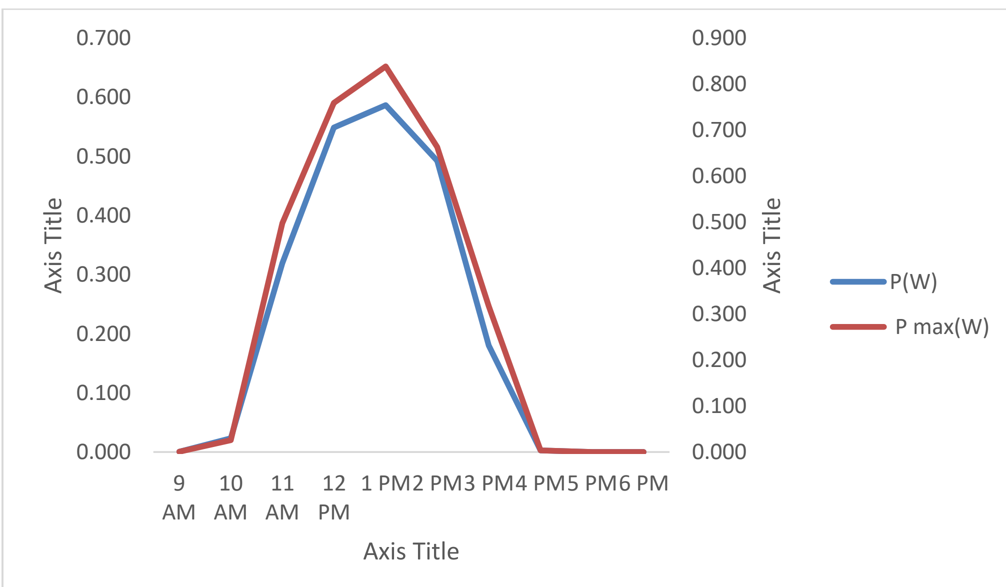

Figure 4.14: Hourly averages variation of power output and maximum power of amorphous silicon module as a function of time for the month of January 2015.

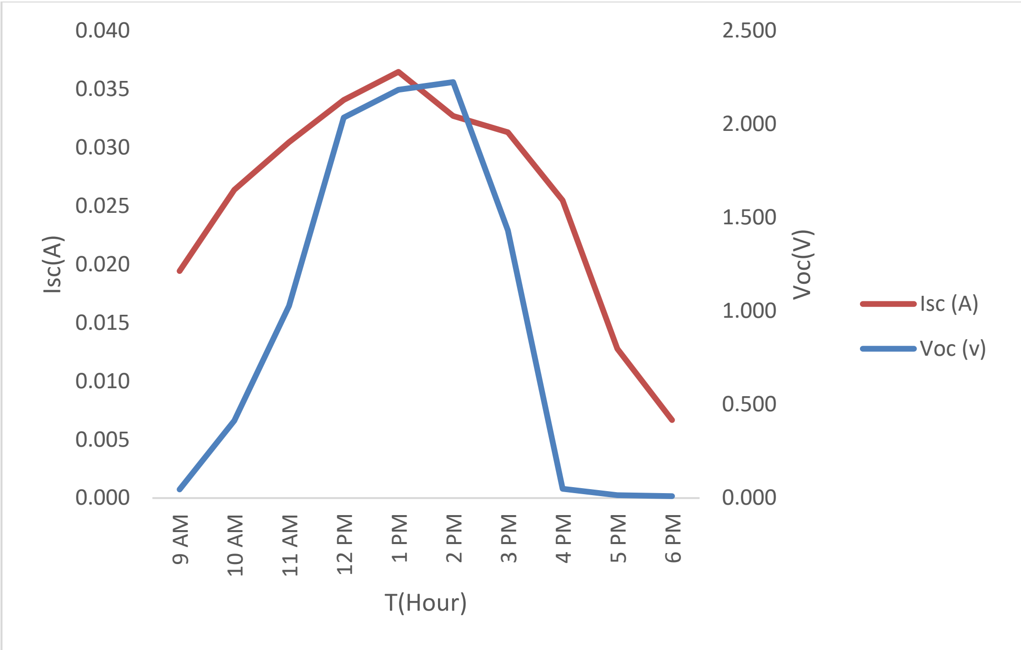

Figure 4.15: Hourly averages variation of short-circuit current and open-circuit voltage of amorphous silicon module as a function of time for the month of August 2015.

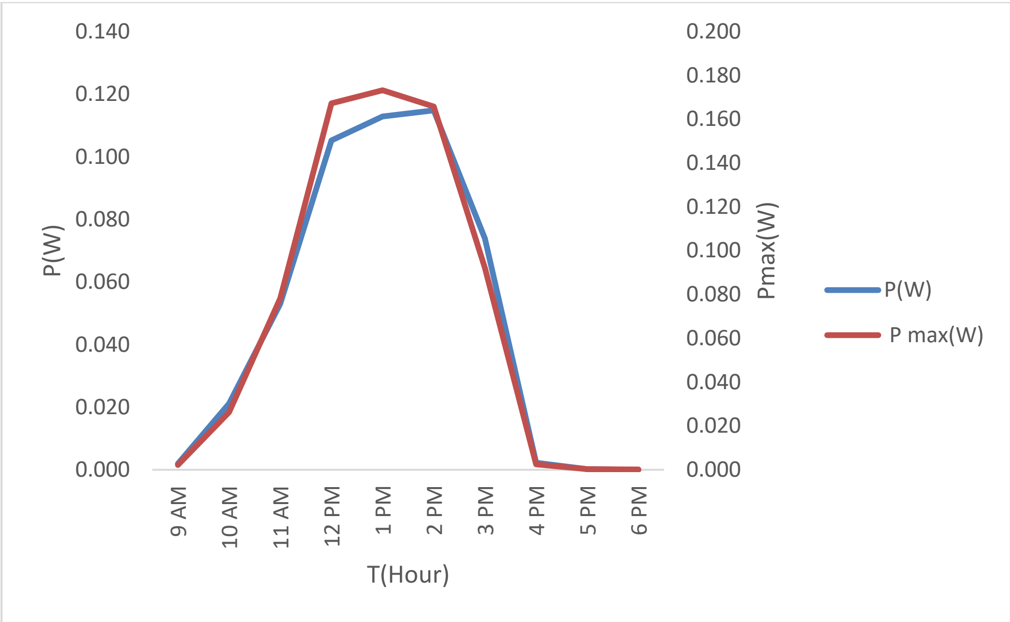

Figure 4.16: Hourly averages variation of power output and maximum power of amorphous silicon module as a function of time for the month of August 2015.

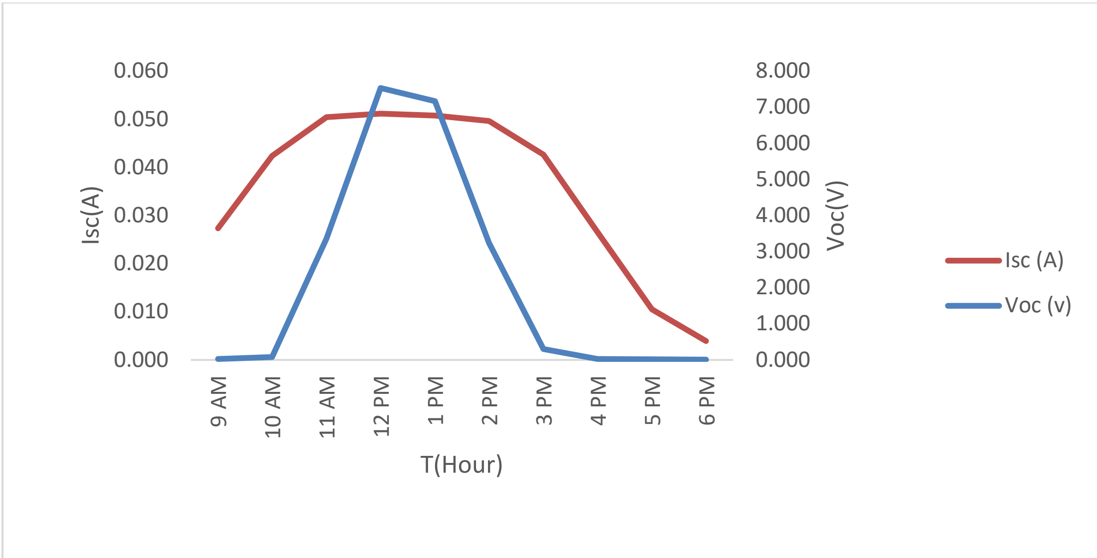

Figure 4.17: Hourly averages variation of short-circuit current and open-circuit voltage of amorphous silicon module as a function of time for the month of January 2016.

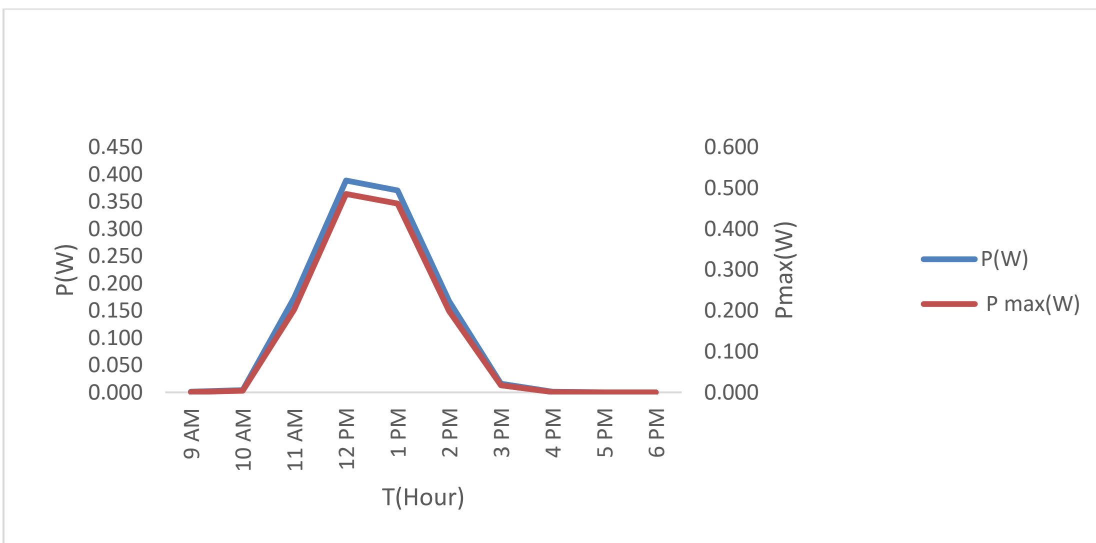

Figure 4.18: Hourly averages variation of power output and maximum power of amorphous silicon module as a function of time for the month of January 2016.

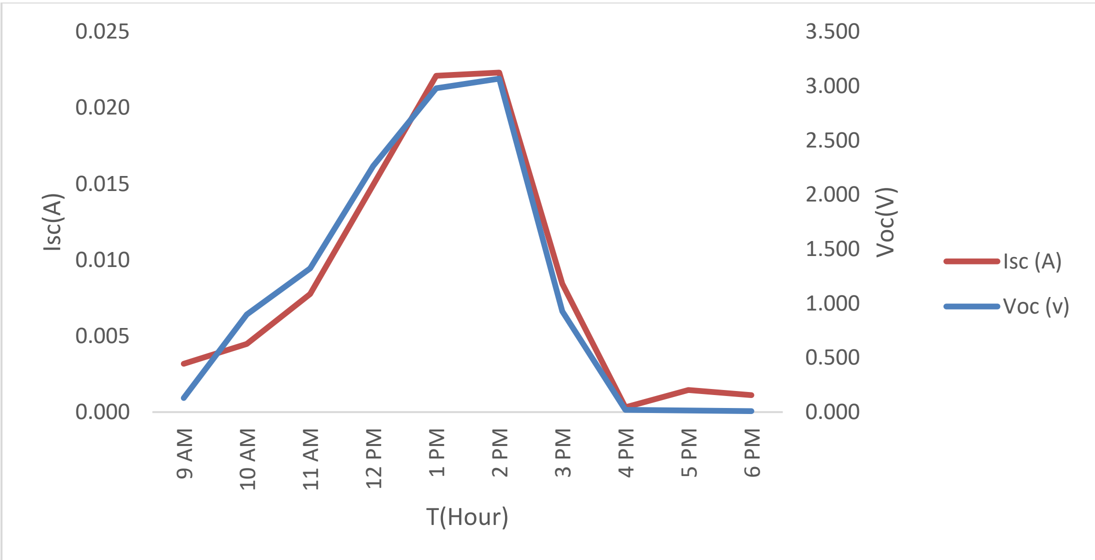

Figure 4.19: Hourly averages variation of short-circuit current and open-circuit voltage of amorphous silicon module as a function of time for the month of August 2016.

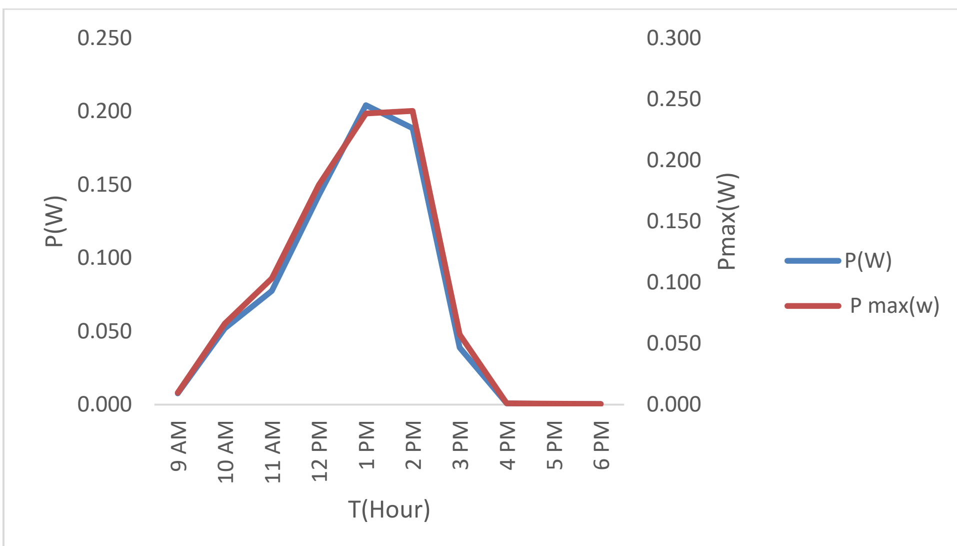

Figure 4.20: Hourly averages variation of power output and maximum power of amorphous silicon module as a function of time for the month of August 2016.

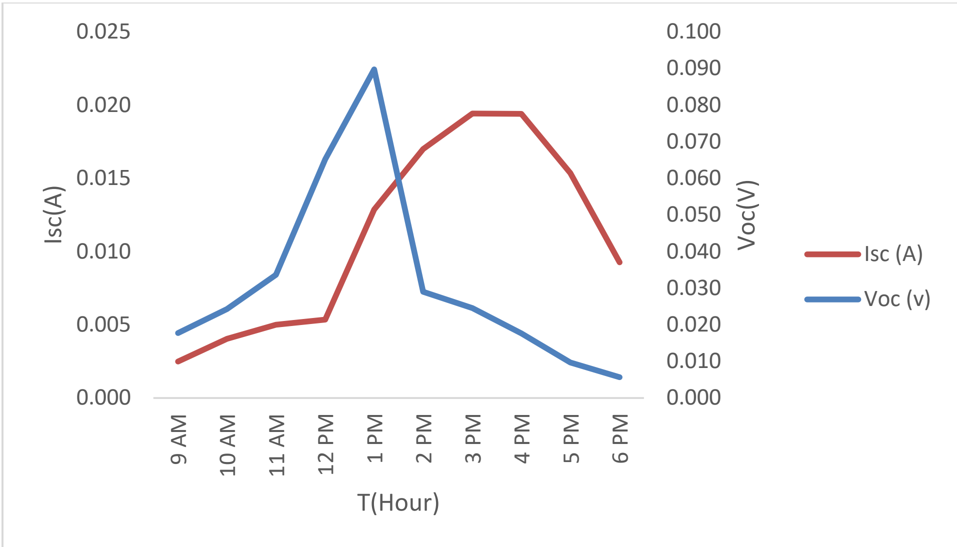

Figure 4.21: Hourly averages variation of short-circuit current and open-circuit voltage of amorphous silicon module as a function of time for the month of January2017.

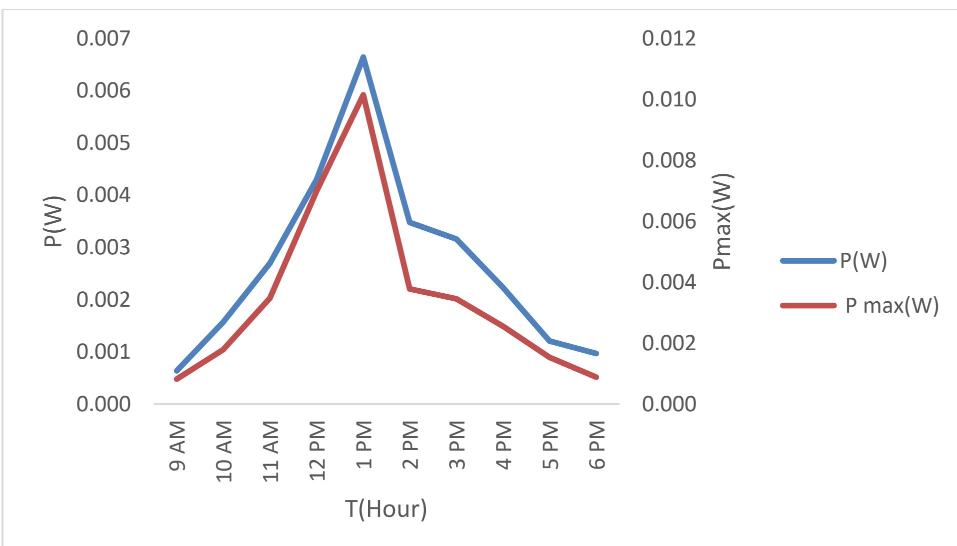

.

Figure 4.22: Hourly averages variation of power output and maximum power of amorphous silicon module as a function of time for the month of January 2017.

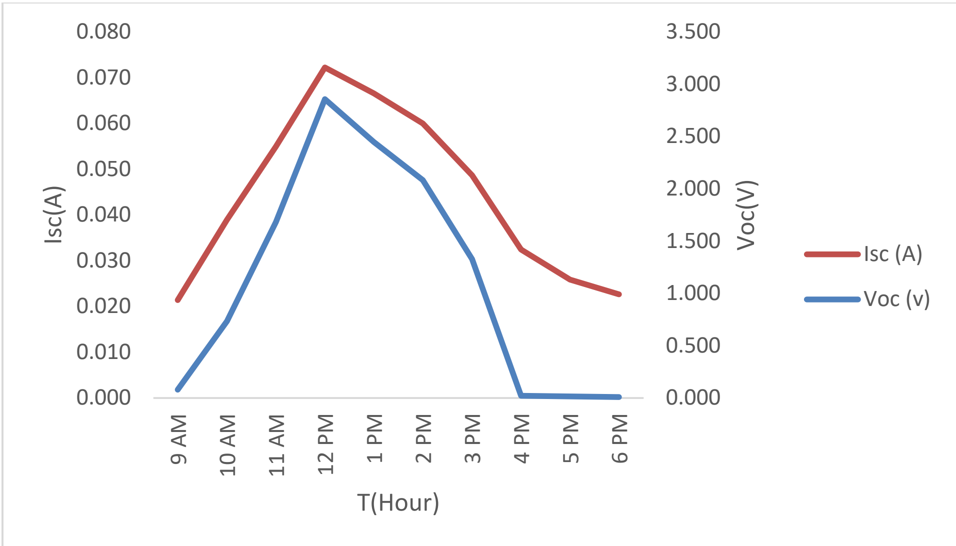

Figure 4.23: Hourly averages variation of short-circuit current and open-circuit voltage of amorphous silicon module as a function of time for the month of August 2017.

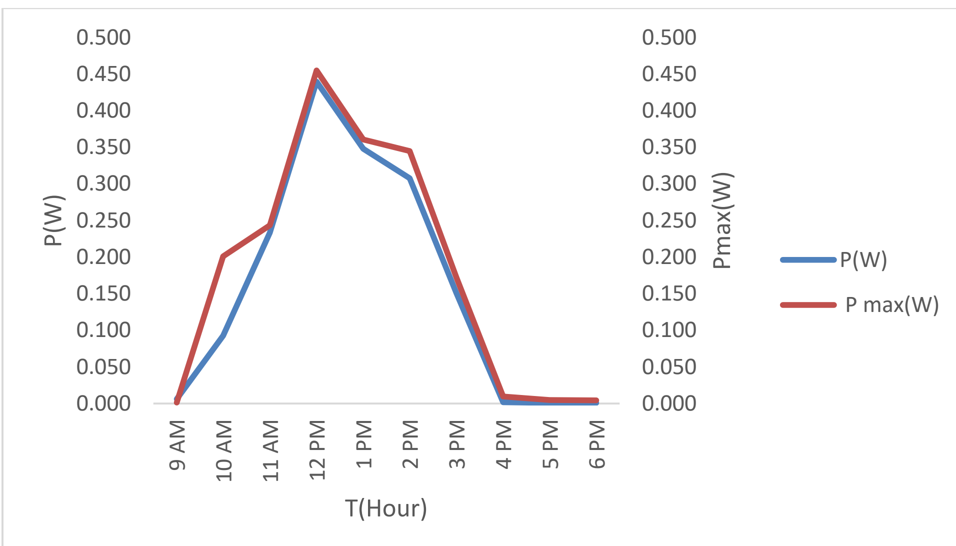

Figure 4.24: Hourly averages variation of power output and maximum power of amorphous silicon module as a function of time for the month of August 2017.

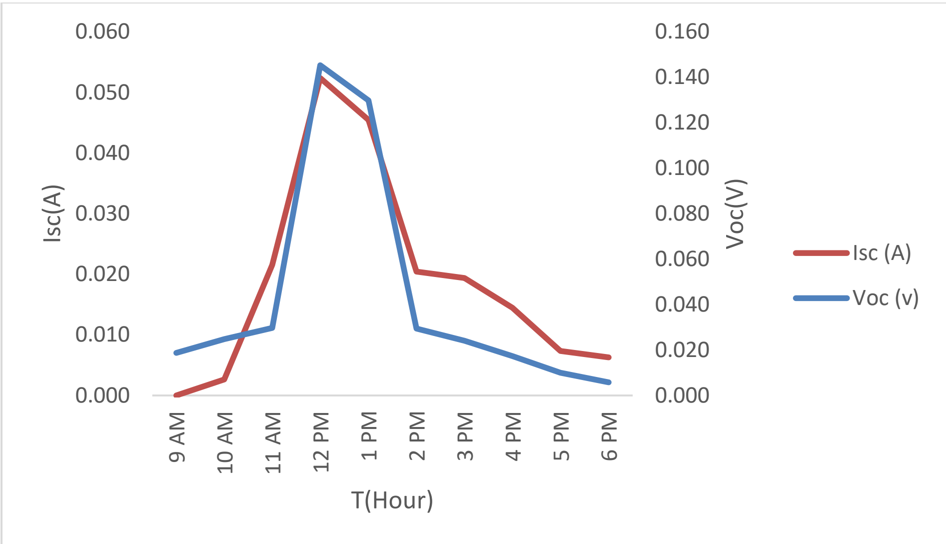

Figure 4.25: Hourly averages variation of short-circuit current and open-circuit voltage of amorphous silicon module as a function of time for the month of January 2018.

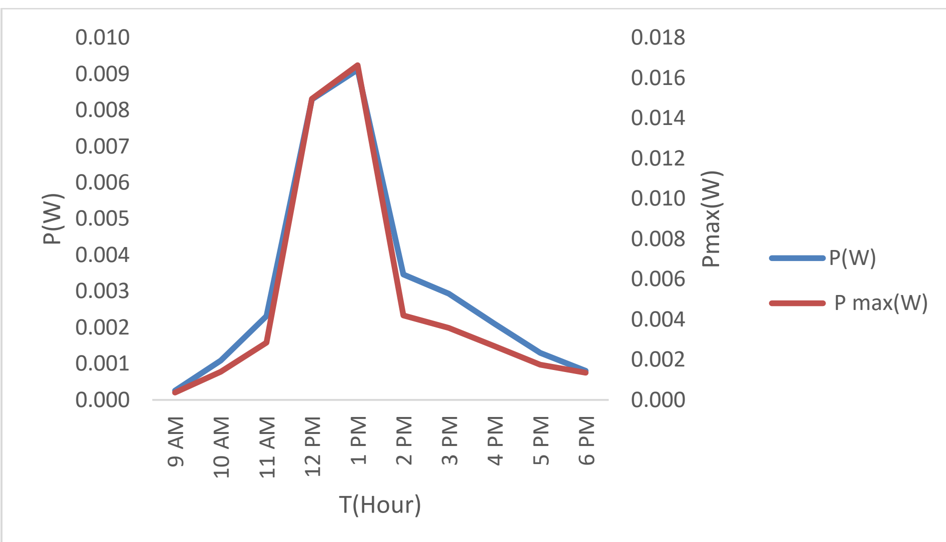

Figure 4.26: Hourly averages variation of power output and maximum power of amorphous silicon module as a function of time for the month of January 2018.

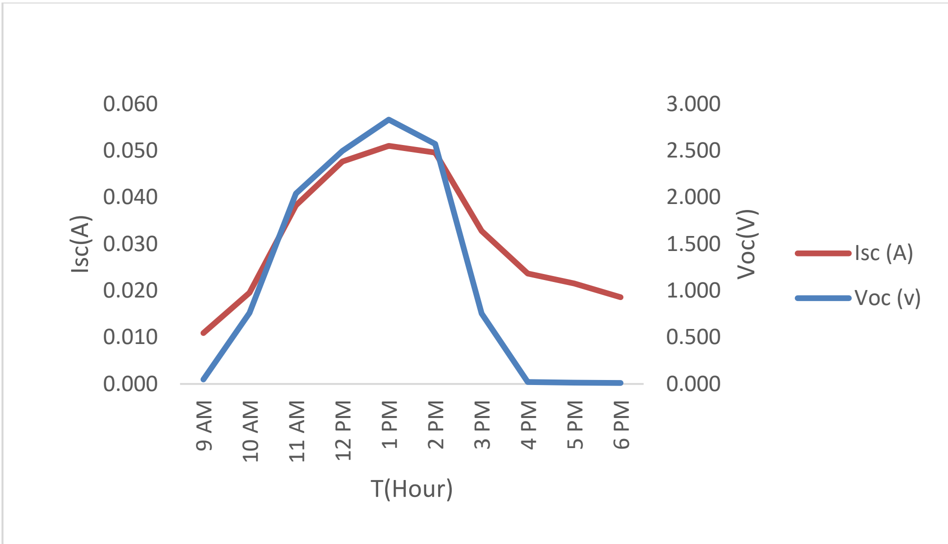

Figure 4.27: Hourly averages variation of short-circuit current and open-circuit voltage of amorphous silicon module as a function of time for the month of August 2018.

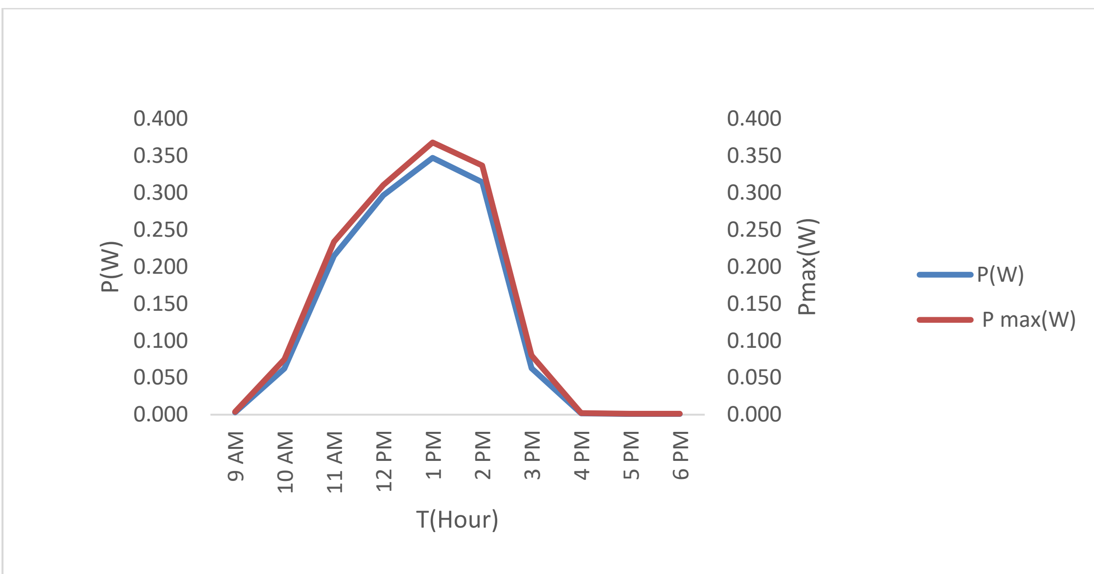

Figure 4.28: Hourly averages variation of power output and maximum power of amorphous silicon module as a function of time for the month of August 2018.

It was observed from the plots of Figures 4.13 – 4.28 that for the four years of study, the amorphous silicon photovoltaic module performance variables peaked at the afternoon time for the two climatic seasons, that is, between 12:00pm and 2:00pm local time which is usually the peak time for amorphous silicon module and this has confirmed the work of Ezenwora, (2016) which states that amorphous silicon module performance variables are usually less affected by high temperature.

The performance responses of amorphous silicon photovoltaic module for the period of four years study at different levels of irradiance (global irradiance) were summarized in Table 4.5. Fill factor and efficiency at the different irradiance levels for the amorphous module were computed and inserted.

Table 4.5: Performance response for year 2015 at different irradiance levels

Hg(W/m^2)	Voc(V)	Isc (A)	Pmax(W)	Vmax(V)	Imax(A)	FF	EFF(%)
276	0.03	0.035	0.001	0.025	0.036	1.029	0.01
375	0.04	0.047	0.002	0.035	0.048	0.894	0.02
437	4.26	0.055	0.222	4.261	0.052	0.946	1.76
537	10.98	0.065	0.558	10.980	0.051	0.785	3.61
643	13.03	0.075	0.670	13.030	0.051	0.680	3.58
743	13.56	0.085	0.707	13.560	0.052	0.612	3.29
835	13.76	0.091	0.718	13.760	0.052	0.571	2.96
912	11.83	0.077	0.601	11.830	0.051	0.662	2.29
933	12.29	0.079	0.641	12.290	0.052	0.658	2.37
1000	12.50	0.080	0.652	12.500	0.052	0.650	2.25

T_{mod} = 37°C, MPR = 0.07, P_{max}(%) = 6.52%

Table 4.6: Performance response for year 2016 at different irradiance levels

Hg(W/m^2)	Voc(V)	Isc (A)	Pmax(W)	Vmax(V)	Imax(A)	FF	EFF(%)
276	0.03	0.039	0.001	0.040	0.013	0.529	0.01
375	0.03	0.039	0.001	0.030	0.039	1.000	0.01
437	3.31	0.035	0.109	3.310	0.033	0.943	0.86
537	7.82	0.045	0.044	10.820	0.004	0.126	0.29
643	8.88	0.055	1.661	8.880	0.187	3.400	8.94
743	8.11	0.065	0.368	5.841	0.063	0.698	1.71
835	8.74	0.075	0.559	8.740	0.064	0.853	2.32
912	10.30	0.075	0.680	10.300	0.066	0.880	2.58
933	11.21	0.085	2.674	12.210	0.219	2.806	9.92
1000	11.61	0.089	2.186	11.750	0.186	2.115	7.56

T_{mod} = 37°C, MPR = 0.23, P_{max}(%) = 21.86%

Table 4.7: Performance response for year 2017 at different irradiance levels

Hg(W/m^2)	Voc(V)	Isc (A)	Pmax(W)	Vmax(V)	Imax(A)	FF	EFF(%)
276	0.02	0.023	0.003	0.020	0.152	6.609	0.04
375	0.03	0.029	0.004	0.025	0.167	5.759	0.04
437	2.91	0.034	0.422	2.910	0.145	4.265	3.34
537	9.52	0.044	0.733	9.520	0.077	1.750	4.72
643	12.21	0.055	1.233	12.210	0.101	1.836	6.64
743	10.32	0.067	1.744	10.320	0.169	2.522	8.12
835	11.48	0.077	1.573	11.480	0.137	1.779	6.52
912	11.74	0.071	2.160	11.740	0.184	2.592	8.20
933	12.45	0.088	2.303	12.450	0.185	2.102	8.54
1000	11.70	0.088	2.078	11.740	0.177	2.018	7.19

T_{mod} = 38.6°C, MPR = 0.22, P_{max}(%) = 20.78%

Table 4.8: Performance response for year 2018 at different irradiance levels

Hg(W/m^2)	Voc(V)	Isc (A)	Pmax(W)	Vmax(V)	Imax(A)	FF	EFF(%)
276	0.02	0.084	0.000	0.011	0.025	0.218	0.00
375	0.02	0.038	0.002	0.025	0.081	2.664	0.02
437	5.33	0.048	0.117	5.330	0.022	0.458	0.93
537	8.60	0.058	1.634	8.600	0.190	3.276	10.53
643	8.78	0.068	1.730	8.780	0.197	2.897	9.31
743	8.43	0.077	1.585	8.430	0.188	2.442	7.38
835	10.33	0.089	0.282	2.372	0.119	0.307	1.17
912	11.50	0.146	1.679	11.500	0.146	1.000	6.37
933	11.77	0.091	2.024	11.770	0.172	1.890	7.51
1000	12.24	0.080	1.812	12.240	0.148	1.850	6.27

T_{mod} = 38.4°C, MPR = 0.19, P_{max}(%) = 18.12%

The module performance for the four years of study was compared with Standard Test Condition (STC) specifications. The maximum power achieved at 1000W/m^2 for the four years of study are 0.652W, 2.186W, 2.078W, and 1.812W representing 6.52%, 21.86%, 20.78% and 18.12% of the manufacturer's 10W specification. Module efficiency at 1000W/m^2 for the four years of study is 2.25%, 7.56%, 7.19%, and 6.27% respectively as against the manufacturers STC specification of 33%. The Open voltage at 1000W/m^2 recorded 12.5V, 11.6V, 11.7V and 12.2V as against the manufacturers STC specification of 21.2V for the four years of study while the short circuit currents are 0.08A, 0.09A, 0.09A and 0.08A as against the manufacturers STC specifications of 0.62A for the four years of study. Similarly, maximum voltage (V_{max}) which according to manufacturers STC specification is 17.4V, recorded 12.5V, 11.8V, 11.74V and 12.2V at 1000W/m^2 for the first, second, third and fourth year respectively, while the maximum current (I_{max}) recorded 0.05A, 0.19A, 0.18A and 0.15A for the four years of study as against the manufacturers specification of 0.55A. Module performance ratios for the amorphous silicon module under investigation for the four years of study are 0.07, 0.23, 0.22 and 0.19 respectively. It was equally observed that no year recorded module temperature of 25^{o}C at 1000W/m^2 solar irradiance as usually assumed for STC conditions as seen in Tables 4.5 for the four years of study. They all recorded module temperature (T_{mod}) well beyond 25^{o}C in the local environment. This four years study of amorphous module has also corroborated the works of Ezenwora, (2016). This clearly shows that there is an enormous margin of deviation of the characterised values from the manufacturers STC specifications, and the STC data is a suspect as the above assertion was equally observed by Car (2005). Therefore designing with manufacturer's STC data will produce an unreliable and defective amorphous photovoltaic power system in Minna.

Annual yearly averages of performance variables and ambient parameters are shown in Table 4.9 for amorphous silicon module to ascertain the average annual Rate of Degradation (RoD).

Table 4.9: Annual yearly averages of performance variables and ambient parameters for the amorphous module.

T(Years)	V_{oc}(V)	I_{sc} (A)	P(W)	P_{max}(W)	T_{mod}(^{0}C)	H_g(W/m^2)	T_a(^{0}C)	WS(m/s)	RH(%)
YEAR 1 (2015)	3.21	0.038	0.173	0.244	35.4	507	25.4	1.65	48.3
YEAR 2 (2016)	2.55	0.031	0.221	0.277	35.5	520	31.4	1.57	49.7
YEAR 3 (2017)	1.76	0.014	0.206	0.237	36.4	502	32.3	1.34	47.1
YEAR 4 (2018)	1.84	0.001	0.141	0.185	36.1	485	32.7	1.03	53.1

Table 4.10: Annual Average Rate of Degradation (RoD) of performance variables for the amorphous module

T(Years)	V_{oc} (V)	I_{sc} (A)	P(W)	Pmax(W)
2015 to 2016	0.66	0.007	0.048	0.033
2016 to 2017	0.79	0.017	0.015	0.040
2017 to 2018	0.08	0.013	0.065	0.052
AVERAGE RoD	0.73	0.010	0.040	0.050

From Table 4.10, it was observed that V_{oc} and I_{sc} has a yearly decrease of 0.66V and 0.007A from year 2015 to 2016, 0.79V and 0.017A from 2016 to 2017, 0.013A for I_{sc} from 2017 to 2018 and a slight increase of 0.08V from 2017 to 2018 for V_{oc}. Furthermore, no decrease was noticed for P and P_{max}in the first year, but rather a slight increase of 0.048W and 0.033W from year 2015 to 2016 was seen. It was discovered that P and P_{max}decreased by 0.015W and 0.04W from 2016 to 2017, 0.065W and 0.052W from 2017 to 2018 suggesting that P and P_{max} began degrading steadily after year 2016. Annual average Rate of Degradation (RoD) for the four years was computed for only the performance variables which reveals that Voc, I_{sc}, P and P_{max} has an annual average RoD of 0.73V, 0.010A, 0.040W and 0.050W respectively for the four years of study as shown in Table 4.10 above. Annual yearly average plots of the performance variables are shown in Figures 4.29 and 4.30

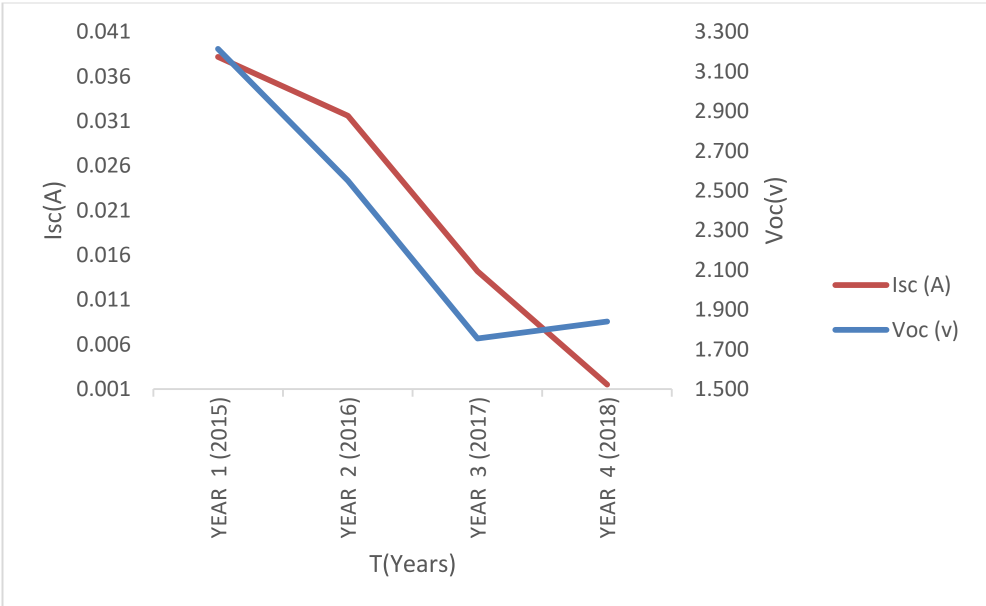

Figure 4.29: Variation of short circuit current and open circuit voltage as a function of years

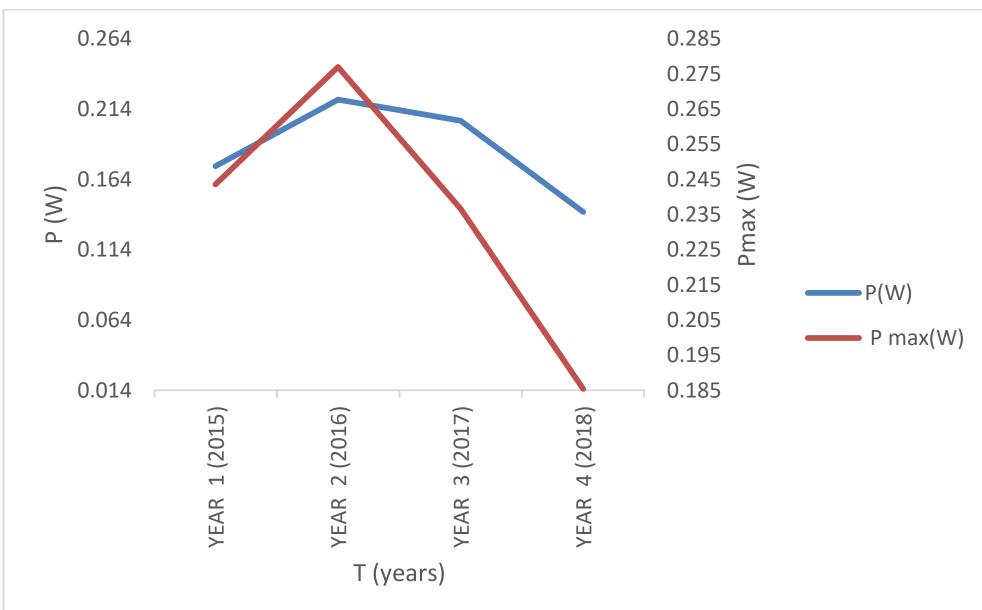

Figure 4.30: Variation of power output and maximum power as a functionof years

Figure 4.29 and 4.30shows the degradation rate for the performance variables being investigated. It was discovered that short- circuit current(Isc) and open-circuit voltage (V_{oc}) decreased steadily from year 2015 to 2018. However, it was observed that the degradation trend was distorted in

2018 where V_{oc} was high. This is due to the fact that according to earlier work of Ezenwora (2016),V_{oc} are known to be affected negatively by high module temperature which accounted for the sudden increase of V_{oc}in year 2018 when a decrease in module temperature was noticed as shown in Table 4.9. The other parameters worthy of note are power (P) and maximum power (P_{max}). From the plots of Figure 4.30, it was observed that there was an increase from 2015 to 2016 before it starts decreasing. The reason for the increase in the first year is not farfetched, according to Ezenwora *et al*.(2018) and other researchers in thisfield, increase in solar irradiance (Hg) and module temperature (T_{mod}) increases P_{max}, and P. Therefore, increase in Hg and T_{mod} as seen in Table 4.9 has accounted for the increase noticed for the P and P_{max} in the first year.

4.2 Statistical Analysis and Models

The data collected for this research work was experimental data over four year period from 2015 to 2018. Minitab version 17 statistical software and Microsoft Excel was used to analyse the data. Both descriptive and inferential statistics was used in analysing the data, Regression model of three variables which include Voc(V), Isc(A) and P (W) was regressed over the four years. A 20 years forecast from the model was derived to determine whether there is downward or upward trend of the experimental data.

4.2.1 Descriptive statistics: Voc (v), Isc (A), Power(W)

The Mean, Standard Error Mean(SE, Mean), Standard deviation (StDev), Variance and Sum of squares of the variables was obtained as in Table 4.11.

Table 4.11: Mean, SE Mean, Standard deviation and Variance

Variable	Mean	SE Mean	St Dev	Variance	Sum	Sum of Square
Voc(v)	2.125	0.358	2.266	5.134	84.99	380.805
Isc(A)	0.02405	0.0029	0.01832	0.000336	0.962	0.03623
P(W)	0.1683	0.0287	0.1815	0.033	6.732	2.4181

From Table 4.11, the mean of Voc(V) was 2. 125 which was higher than the mean of Isc (A) and P (W) with variance of 5.134 and Standard Error of 0.358 (36%), Isc (A) has mean of 0.02405 with variance of 0.0034 and standard Error of 0.0029 (0.3%), while, P (W) has the mean of 0.1683, variance of 0.0330 and Standard Error of 0.0287 (3%) respectively.

4.2.2 Inferential statistics

A multiple regression model was developed with three independent variables which include Voc (V), Isc (A) and P (W) and one dependent variable Years. The Regression equation model for the research work is

YEAR = 3.36 - 0.237 V_{oc} (v) - 71.5 I_{sc} (A) + 8.07 P (W)(4.1)

From equation 4.1, for every unit increase in Voc (V) there is 0.237decrease in the years value keeping Isc (A) and Power (W*)* constant. For every unit increase in Isc (A*)* there is 71.5decrease in the Year's value keeping Voc (V) and Power (W) constant which shows very fast downward trend of the valuesthan the Voc (V). Also for every unit increase in P (W)there is 8.07 increase in the Year'svalue keepingVoc(V) and Isc (A) constant. The percentage decrease of Isc (A) contributed to the fast decrease in the values as the years increases.

Table 4.12 Coefficients of variables (Coef); T-test and P-value

Predictor	Coef	SECoef	T	P	VIF
Constant	3.3639	0.1952	17.23	0	
Voc (v)	-0.2367	0.1381	-1.71	0.095	7.1
Isc (A)	-71.46	11.27	-6.34	0	3.1
Power (W)	8.067	1.679	4.81	0	6.7

From Table 4.12, Since P-values for Isc (A) and Power (W) = 0.000 is less than 0. 05 (5%) the two variables contribute significantly to the model while Voc with P-value -0.095 greater than 0.05 (5%) does not contribute positively to the model. Further, analysis ofvariance explained the significant difference in the contribution of the variables to the model.

Table 4.13: Analysis of variance (ANOVA) for the regression equation

Source of Variance	**Degree of Freedom**	**Sum of Squares**	**Mean Squares**	**F-value**	**P- value**
Regression	3	30.518	10.173	18.80	
0.000					
Residual Error	36	19.482	0.541		
Total	39	50.000			

S = 0.735635 R-Sq = 61.0% R-Sq(adj) = 57.8% R-Sq(pred) = 55.33%

From Table 4.13, Since the P-value = 0.000 is less than 0.05 (5%) level of significant, we shall conclude that there is statistical significant difference in the contributions of the variables to the model with 61% explaining the difference and 39% unexplained. The implication of downward trend of the yearly values shows that there is significant yearly Rate of Degradation (ROD) of the amorphous module.

4.3 Forecasting

A 20 years forecasting of the performance variables used for this study was done using the model developed and tabulated with the predicted values as in Table 4.14

Table 4.14:A twenty (20) years forecasting table

Years	**2019**	**2020**	**2021**	**2022**	**2023**	**2024**	**2025**	**2026**	**2027**	**2028**
Predicted Values	**-53.59**	**-117.25**	**-180.92**	**-244.59**	**-308.26**	**-371.92**	**-435.59**	**-499.26**	**-562.92**	**-626.59**
Years	**2029**	**2030**	**2031**	**2032**	**2033**	**2034**	**2035**	**2036**	**2037**	**2038**
Predicted Values	**-690.26**	**-753.92**	**-817.59**	**-881.26**	**-944.93**	**-1008.59**	**-1072.26**	**-1135.93**	**-1199.59**	**-1263.26**

Figure 4.31: Shows the line graph of the downward trend of the predicted values over a 20 years period

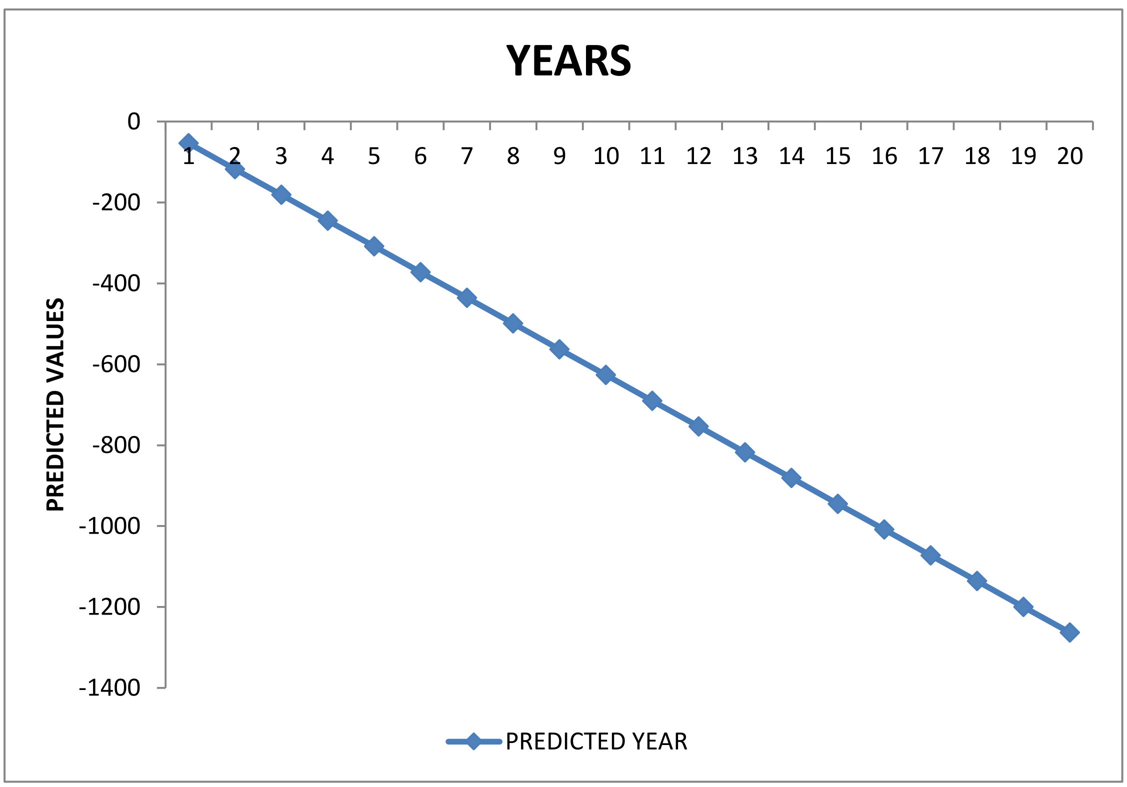

Figure 4:.31Line graph of the predicted value for the performance variables

Keys:

- Year 1 = 2019
- Year 2 = 2020
- Year 3 =2021
- Year 4 =2022
- Year 5 =2023
- Year 6 =2024
- Year 7 =2025
- Year 8 =2026
- Year 9 =2027
- Year 10 =2028
- Year 11 =2029
- Year 12 = 2030
- Year 13 =2031
- Year14 =2032
- Year 15 =2033
- Year 16 =2034
- Year 17 =2035
- Year 18 =2036
- Year 19 =2037
- Year 20 =2038

CHAPTER FIVE

5.0 CONCLUSION AND RECOMMENDATION

5.1 Conclusion

The outdoor characterisation and performance evaluation of amorphous silicon photovoltaic module in Minna local environment for the four years study period reveals that the actual values of performance variables of the module differ greatly from the manufacturer's specifications. The maximum power achieved at 1000W/m^2 for the four years of study are 0.652W, 2.186W, 2.078W, and 1.812W representing 6.52%, 21.86%, 20.78% and 18.12% of the manufacturer's 10W specification. Module efficiency at 1000W/m^2 for the four years of study is 2.25%, 7.56%, 7.19%, and 6.27% respectively as against the manufacturers STC specification of 33%. Similarly, it was equally observed that no year recorded module temperature of 25^{o}C at 1000W/m^2 irradiance as used in STC specifications by the manufacturer. Instead, the four years study recorded module temperature (T_{mod}) well beyond 25^{o}C in the local environment. This clearly shows that there is an enormous margin of deviation of the characterised values from the manufacturers STC specifications, and the STC data is a suspect as the above assertion was equally observed by Car (2005). Therefore designing with manufacturer's STC data will produce an unreliable and defective amorphous photovoltaic power system.

The yearly determination of Rate of Degradation (RoD) of amorphous photovoltaic modules in Minna local environment reveals that all the performance variables of the module degraded significantly from year to year for the four years of study. It reveals thatV_{oc}, I_{sc}, P and P_{max}has an annual average RoD of 0.73V, 0.010A, 0.040W and 0.050W respectively for the four years of study. Similarly, It was observed that V_{oc} and I_{sc} has a yearly decrease of 0.66V and 0.007A from year 2015 to 2016, 0.79V and 0.017A from 2016 to 2017, 0.013A for I_{sc} from 2017 to 2018 and a slight increase of 0.08V from 2017 to 2018 for V_{oc}. Furthermore, no decrease was noticed for P and P_{max} in the first year, but rather a slight increase of 0.048W and 0.033W from year 2015 to 2016 was seen. It was discovered that P and P_{max} decreased by 0.015W and 0.04W from 2016 to 2017, 0.065W and 0.052W from 2017 to 2018 suggesting that P and P_{max} began degrading steadily after year 2016. Module temperature was therefore observed to have significant influence on the general degradation of the module especially V_{oc}because it has no linear relationship with temperature and solar irradiance hence the increase when temperature decreased in 2018. In addition to the temperature effects on the degradation of the module is solar irradiance which is seen to affect P and$P_{max,}$ hence the increase when temperature and solar irradiance increased in the first year of study.

5.2 Recommendations

Although yearly performance and Rate of Degradation (RoD) has been extensively carried out under Minna prevailing meteorological parameters, however, there are still areas where work needs to be done.

i. Various studies suggest that amorphous module degrade over time after long time of outdoor exposure, only four years study was considered in this work. It is, therefore, recommended that longer years of outdoor exposure be carried out in the Minna local environment.

ii. Dust accumulation is known to have significant effect on the degradation of PV modules and Minna local environment is situated within the semi-arid part of the Sahel region of Northern Nigeria where Harmattan dust is endemic during the dry season. This was not considered in this work; hence it should be included in further work in Minna.

iii. It is also recommended that outdoor, yearly degradation studies should be carried out on all commercially available PV modules in every location of developing countries where this is lacking. Results will furnish policy makers, designers, PV power system installers the vital information on the degradation rate and lifespan of all commercially available PV modules for effective and reliable PV power system.

REFERENCES

AgrilInfo.in, (2013): Factors affecting solar radiation. http://www.innovateus.net. (2013), retrieved August 20019.Guide to PV system design and installation, (2001). California energy commission: Energy development division.

Agroui K., Hadj A., Pellegrino M., Giovanni F. &Mahammad I. (2011). Indoor and outdoor photovoltaic modules performances based on thin films solar cells. *Research and Applications. Renewable Energy,* 14: 469-480.

Anuforom, A.C., Akeh, L.E., Okeke, P.N &Opara, F.E., (2007).Inter-annual variability and long-term trend of uv-absorbing aerosols during harmattan season in sub-saharanwest africa. *Atmospheric environment,*41, 1550-1559.

Azhar G. & Abdul M. (2012).The performance of three different solar panels for solar electricity applying solar tracking device under the malysian climate condition.*Energy and environment research*, 2: 235-243.

Akachuku, B. (2011). Prediction of optimum angle of inclination for flat plane solar collector in Zaria, Nigeria.*Agricultural Engineering International Journal, CommisionInternationale du Genie Rural*, 13:1-11.

Bala, E.J., Ojosu, J.O. & Umar, I.H. (2000). Government policies and programmes on the development of the solar PV sub-sector in Nigeria. *Nigeria Journal of Renewable Energy* 8 (1 & 2) pp 1-6.

Carlson, T.N. &Benjamin, S.G., (1980).Radiative heating rates for saharan dust. *Journal of atmospheric science* 37, 193-213.

Carr A. (2005). A detailed performance comparison of pv modules of different technologies and the implications for the pv system design methods. *Phd thesis*; murdock university. Western Australia.

Cornaro, C. &Musella D. (2010). *Performance analysis of pv modules of various technologies after more than one year of outdoor exposure in Rome, Italy.*

Chen, C. J. (2011). *Physics of solar energy*.Hoboken, John Wiley & sons, Inc. p. xv.

Chantelle, R. & Van Dyke, E.E. (2010).Degradation analysis of CIGS photovoltaic modules.*Solar energy material and solar cells,* 94(3), pp617-622.

Duke R., Graham S., Mark H., Arne J., Daniel M., Osawa B., Simone P. & Erika W. (1999). Field performance evaluation of amorphous silicon (a-si) photovoltaic systems in kenya: methods and measurements in support of a sustainable commercial solar energy industry.*A Project of Energy Alternatives Africa (EAA) and Renewable Appropriate*

Energy Laboratory (RAEL) and Energy and Resources Group (ERG), University of California, Berkeley.

Dunlop E. &Halton D. (2006).The performance of crystalline silicon photovoltaic solar modules after 22 years of exposure**.***Progress in photovoltaic. Research applications,* **7**:16-23.

Domenico, C .(2009). Degradation and annealing of amorphous silicon solar cells by current injection experiment and modeling.*Solar energy materials & solar cells*59 (1999) 289-298.

Ezewonra, J.A; (2016).Development of a prototype photovoltaic power system based on characterization and performance evaluation of photovoltaic modules in Minna, Nigeria.*PhD Thesis,Department Of Physics, Federal University of Technology, Minna.*pp 45-140.

Ezewonra, J.A; Oyedum, D.A. &Ugwoke, P.E. (2018).Comparative study on different types of photovoltaic modules under outdoor operating conditions in Minna, Nigeria.*International Journal of Physical Research.* 6(1), pp 35-48.

Kazmerski, L.L. (1980). *Polycrystalline and amorphous thin films and devices*. New York: Academic Press, pp 76-83.

Manuel V. & Ignacio R. (2008).Photovoltaic module reliability model based on field degradation studies. *Progress report on photovoltaics:research and applications,* 10: 825-1002.

Muller, R. S., Kamins, T. I. & Chan, M. (2003).*Device electronics for integrated circuits* (3rd Edition.).Danvers, John Wily & Sons.pp 73.

Mon, G.R. & Ross, R.G. (1985).Electrochemical degradation of amorphous-silicon photovoltaic modules. *Proceedings of the 18th IEEE Photovoltaic Specialists Conference* Las Vagas, Nevada, October 21-25, 1985.

Neville, R.C. (1980). Solar energy conversion-the solar cell.*Elsevier Scientific Publishing Company,* New York.

Ohnishi, M., Kishi, Y., Nakano, S., Kawoda, H., Tsuda, S., Shibuya, H., Tanaka, M. &Kuwano, Y. (1985). High performance a-si solar cells and new fabrication methods a-si solar cells.6th E.C. *Photovoltaic Energy Conference*, London, U.K. pp 71-77.

Quijano, A.L. (2000). Radiative heating and direct radiative forcing by mineral dust in cloudy atmospheric conditions. *Journal of Geophysical Research* 105 (D10), 12,207-12,219.

Rakovect, J. &Klemen, Z. (2011).Orientation and tilt dependence of a fixed PV array energy yield based on measurements of solar energy and ground albedo- A Case Study of Slovenia. *Progress Report on Photovoltaics: Research and Applications,* 13: 42-51.

René, J. (2005). *Introduction to polymer solar cells*.Eindhoven University of Technology, Netherlands. 3Y280.

Rong P., Joseph K. &Govindasamy T. (2011). Degradation analysis of Solar Photovoltaic modules: Influence of environment factor. *In the proceedings of reliability and maintainability symposium*,15: 24-27.

Solmetric (2011).*Guide to interpreting I-V curve measurements of PV arrays*. California, Solmetric Corporation.

Twidell, J. & T. Weir (2006). *Renewable energy resources*. New York: Taylor & Francis.

Van-Dyke, E.E; Audouard, A; Meyer, E.L. &Woolard, C.D. (2006).Investigation of the degradation of a thin-film hydrogenated amorphous silicon photovoltaic module. *Solar energy materials and solar cells* 91 pp 167-173.

Wronski, C.R. (1985). Recent progress of device performance and stability in a-si solar cells.*Technical digest of the international photovoltaic solar energy conference*,Tokyo, Japan, pp 557-563.

Wronski, C.R., Pearce, J.M., Koval, R.J., Ferlauto A.S. & Collins, R.W. (2000).Progress in amorphous silicon-based solar cell technology.*World climate and energy event*,pp 67-72.

Yang, J. (1997).Recent progress on amorphous silicon alloy leading to 13% stable cell efficiency.*Proceedings of 26th IEEE photovoltaic specialist conference*, pp563-568.

APPENDIX A

Descriptive Statistics: Voc (v), Isc (A), Power (W)

Variable	Mean	SE Mean	StDev	Variance	Sum	Sum of Squares
Voc (v)	2.125	0.358	2.266	5.134	84.990	380.805
Isc (A)	0.02405	0.00290	0.01832	0.00033	0.9620	0.03623
Power(W)	0.1683	0.0287	0.1815	0.0330	6.7320	2.4181

Regression Analysis: YEAR versus Voc (v), Isc (A), Power(W)

The regression equation is
YEAR = 3.36 - 0.237 V_{oc} (v) - 71.5 I_{sc} (A) + 8.07 Power(W)

Predictor	Coef	SECoef	T	P	VIF
Constant	3.3639	0.1952	17.23	0.000	
V_{oc} (v	-0.2367	0.1381	-1.71	0 .095	7.1
I_{sc} (A)	-71.46	11.27	-6.34	0.000	3.1
Power(W)	8.067	1.679	4.81	0.000	6.7

S = 0.735635   R-Sq = 61.0%   R-Sq(adj) = 57.8%

PRESS = 22.3372   R-Sq(pred) = 55.33%

Analysis of Variance

Source	DF	SS	MS	F	P
Regression	3	30.518	10.173	18.80	0.000
Residual Error	36	19.482	0.541		
Total	39	50.000			

Durbin-Watson statistic = 0.496199

No evidence of lack of fit (P >= 0.1).

SUMMARY OUTPUT

Regression Statistics	
Multiple R	0.78125896
R Square	0.61036556
Adjusted R Square	0.57789602
Standard Error	0.73563507
Observations	40

ANOVA

	df	*SS*	*MS*	*F*	*Significance F*
Regression	3	30.518278	10.17276	18.7981	1.66237E-07
Residual	36	19.481722	0.541159		
Total	39	50			

	Coefficients	*tandard Errc*	*t Stat*	*P-value*	*Lower 95%*	*Upper 95%*	*ower 95.0%*	*Upper 95.0%*
Intercept	3.36391854	0.1952028	17.23294	5.68E-19	2.968028855	3.759808231	2.968029	3.759808231
Voc (v)	-0.2367122	0.1380733	-1.7144	0.095055	-0.516737794	0.043313321	-0.51674	0.043313321
Isc (A)	-71.458631	11.268123	-6.34166	2.43E-07	-94.31144396	-48.6058183	-94.3114	-48.60581834
Power(W)	8.06664207	1.6787286	4.805209	2.72E-05	4.662022736	11.47126141	4.662023	11.47126141

YEAR = 3.36 - 0.237 V_{oc} (v) - 71.5 I_{sc} (A) + 8.07 Power(W)

YEAR	V_{OC}	I_{SC}	P_W	PREDICTED VALUES
1	3.12	-68.14	11.43	-53.59
2	2.89	-139.64	19.50	-117.25
3	2.65	-211.14	27.57	-180.92
4	2.41	-282.64	35.64	-244.59
5	2.18	-354.14	43.71	-308.26
6	1.94	-425.64	51.78	-371.92
7	1.70	-497.14	59.85	-435.59
8	1.46	-568.64	67.92	-499.26
9	1.23	-640.14	75.99	-562.92
10	0.99	-711.64	84.06	-626.59
11	0.75	-783.14	92.13	-690.26
12	0.52	-854.64	100.20	-753.92
13	0.28	-926.14	108.27	-817.59
14	0.04	-997.64	116.34	-881.26
15	-0.20	-1069.14	124.41	-944.93
16	-0.43	-1140.64	132.48	-1008.59
17	-0.67	-1212.14	140.55	-1072.26
18	-0.91	-1283.64	148.62	-1135.93
19	-1.14	-1355.14	156.69	-1199.59
20	-1.38	-1426.64	164.76	-1263.26

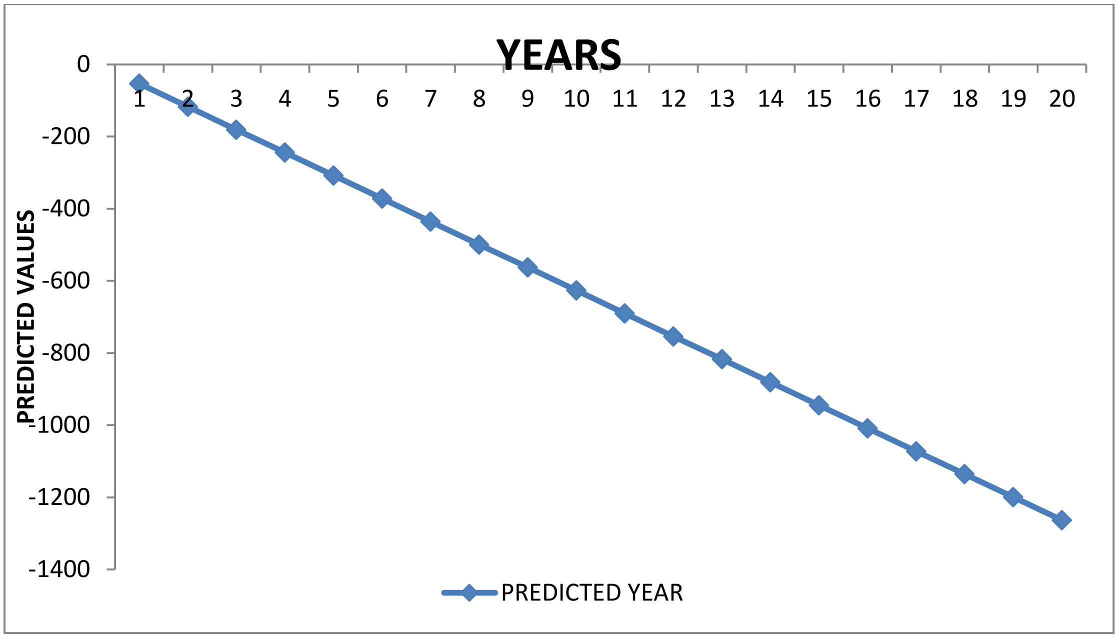

Keys:

- Year 1 = 2019
- Year 2 = 2020
- Year 3 =2021
- Year 4 =2022
- Year 5 =2023
- Year 6 =2024
- Year 7 =2025
- Year 8 =2026
- Year 9 =2027
- Year 10 =2028
- Year 11 =2029
- Year 12 = 2030
- Year 13 =2031
- Year14 =2032
- Year 15 =2033
- Year 16 =2034
- Year 17 =2035
- Year 18 =2036
- Year 19 =2037
- Year 20 =2038